AD-786 155

PACKET RADIO COMMUNICATIONS

F. H. Dickson

Collins Radio Company

Prepared for:

Advanced Research Projects Agency

30 September 1974

DOCUMENT CONTROL DATA - R & D   AD 786 155

(Security classification of title, body of abstract and indexing annotation must be entered when the overall report is classified)

1 ORIGINATING ACTIVITY (Corporate author)	2a. REPORT SECURITY CLASSIFICATION
Collins Radio Company	Unclassified
	2b. GROUP None

3 REPORT TITLE

Quarterly Technical Report for the project "Packet Radio Communications"

4 DESCRIPTIVE NOTES *(Type of report and inclusive dates)*

Quarterly Technical Report

5 AUTHOR(S) *(First name, middle initial, last name)*

Collins Radio Company

6 REPORT DATE	7a. TOTAL NO. OF PAGES	7b. NO. OF REFS
	80	3

8a. CONTRACT OR GRANT NO	9a. ORIGINATOR'S REPORT NUMBER(S)
DAHC15-73-C-0192	
b. PROJECT NO	523-0699813-001C3L
ARPA Order No. 2305	
c.	9b. OTHER REPORT NO(S) *(Any other numbers that may be assigned this report)*
d.	

10 DISTRIBUTION STATEMENT

Distribution of this document is unlimited.

11 SUPPLEMENTARY NOTES	12 SPONSORING MILITARY ACTIVITY
	Advanced Research Projects Agency, Department of Defense

13 ABSTRACT

Three major areas of activities in support of packet radio communications are reported in this document. These are: (1) Analysis of the pseudorandom code spread spectrum technique, (2) evaluation and selection of the pseudorandom codes for the experimental repeater, and (3) development of a signal capture model. The analysis of the code spread spectrum includes considerations of synchronization and multiple access capabilities. The code selection is based on the computer-derived side lobe properties and crosscorrelation of high data rate codes with low data rate codes. The developed capture model is based on the repeater design currently being developed and will be used to model capture in the existing packet radio network simulation models, which presently have no capture. Also, a brief status report of the repeater equipment development is included in the introduction.

DD FORM **1473**
1 NOV 65

Unclassified

14 KEY WORDS	LINK A		LINK B		LINK C	
	ROLE	WT	ROLE	WT	ROLE	WT
Packet radio communications, spread spectrum, multiple access, data communications, synchronization, Golay codes, capture.						

COLLINS

quarterly technical report

Packet Radio Communications
Collins Radio Company

Principal Investigator:
F.H. Dickson
(214) 235-9511

SUMMARY

A. TECHNICAL PROBLEM

This project is one part of a larger effort directed at extending packet switching technology into the area of radio communications. The technical investigations are focused on a Packet Radio Network to serve fixed and mobile digital terminals in a tactical command and control environment. The objectives of the Collins investigations are:

- Perform research covering the application of radio frequency technology to packet switched communications.

- Participate in the overall ARPA Packet Communications Technology Program under the guidance of the Packet Radio Communications Working Group.

- Develop experimental equipments to support the Packet Radio System/Network experiments.

- Recommend a system architecture to provide terminal-to-terminal security for the packet switched radio network.

B. GENERAL METHODOLOGY

The approach to the packet radio investigations is a combination of theoretical studies, equipment design efforts, and laboratory experiments. Work has been directed at each of the following areas:

- Experimental Equipment Design and Build. Detailed design and assembly of the experimental repeater described in the last quarterly report, "Technical Plan for the Packet Radio Experimental Repeater," July 1974.

- Modulation and Detection. Investigation of modulation schemes and signal processing techniques as related to contention, channelization, and coexistence properties.

- Communications Security. Evaluation of the impact of encryption and traffic flow security requirements and disciplines on system design.

The above studies and design efforts are organized as an interactive process to achieve a proper balance between system performance and the constraints of available technology.

C. TECHNICAL RESULTS

This quarterly report treats three primary topics which have been investigated during the reporting period in support of the experimental packet radio repeater development. Specific technical results reported include the following:

- Pseudonoise Spread Spectrum Modulation. Detailed consideration of pseudonoise spread spectrum (PNSS) techniques, including coexistence considerations.

- Code Selection. Description of an optimization program for selecting the Golay code sequences to be used for MSK modulated code spread spectrum signaling in the experimental repeater.

- Capture Model Description. Characterization of the ability of the experimental repeater receiver design to distinguish and lock onto one signal from an ensemble of several simultaneous signals.

In addition, substantial progress has been made in the detailed design and development of the experimental packet radio repeater. Breadboards of most circuit functions have been built and are being tested. Printed circuit boards/modules are under development.

The report of work done in communications security is reported in other documents.

D. PLAN FOR NEXT QUARTER ACTIVITIES

The emphasis during the next quarter will be on the continued design and integration of the experimental repeater. Circuit design and layout will be completed; modules and circuit boards will continue to be fabricated, assembled, and tested; and the radio and digital subsections of the experimental repeater will be integrated. Extensive tests will be run at this level to thoroughly evaluate the overall performance of the experimental repeater design prior to final assembly, test, and integration of the initial experimental units into the packet radio experimental test bed.

A spread spectrum mode of signaling has been selected for the experimental repeater for the ARPA packet radio project. The choice was made because the processing gain associated with the expanded bandwidth resulting from the use of spread spectrum techniques can be used to provide a degree of "capture" for the multiple access channel or some protection against interfering signals. The use of the spread spectrum techniques also reduces the effect of the packet radio signals on other systems operating in the same general frequency band.

This report presents the results of several studies of pseudonoise spread spectrum modulation techniques and their use in the experimental repeater now under development for the ARPA packet radio project. Section 2 is a detailed discussion of pseudonoise spread spectrum modulation. Performance advantages with respect to operation in the presence of strong interfering signals, such as jamming signals, coexistence, multipath rejection, and multiple access to a single channel, are discussed. Section 3 is a description of an optimization program developed for selecting Golay code sequences to be used for MSK modulated code spread spectrum signaling in the experimental repeater. Finally, Section 4 contains a characterization of the expected signal capture capability of the experimental repeater, that is, the ability of the receiver to distinguish and lock onto one spread spectrum radio signal from an ensemble of several simultaneous signals.

In addition to the work described above, substantial progress has been made on the development of the experimental packet radio repeater. Breadboards of most of the radio section circuits have been completed pursuant to the technical plan (published in the last quarterly report) and are undergoing test. Completed breadboards include the encoder/modulator, the rf head (up-converter, power amplifier, T/R switch, and down-converter), the noncoherent agc, the coherent agc, EOP/data detector, and the bit sync. In addition, printed circuit board modules are under development for most of these functions. A completed prototype module is available for the frequency generator. With respect to the digital section, printed circuit boards for the random access memory and the programmable read only memory have been built and tested.

The following modules have been designed and are in printed circuit board layout: CPU (including timing), address decode, DMA channels, and the receive interface. The repeater software development is proceeding according to plan. The following program elements are designed and ready for debugging:

a.   Executive Program

b.   Interrupt Process Routines

c.   Software/System Development (Debug Aids) Program

d.   Paper Tape Load/Dump Routines

e.   Terminal I/O Routines

f.   Initialization/Restart Program.

Development plans are being formulated for the radio interface software and digital hard-ware test software elements.

Pseudonoise Spread Spectrum Analysis

2.1 INTRODUCTION

The ARPA experimental repeater utilizes a pseudonoise spread spectrum (PNSS) signaling technique. This section of the quarterly report is a tutorial discussion of this spread spectrum approach. In the experimental repeater minimum shift keying (MSK), which can be defined as phase continuous FSK with a modulation index equal to 0.5, is used to modulate the carrier. The reasons for this choice are delineated in the Experimental Repeater Design Plan. The more classic modulation technique, PSK, is used throughout this section of the report. This was done to enable the reader to concentrate on the spectrum spreading discussion itself and not be encumbered with the additional conceptual complexities of MSK. The fundamental characteristics and properties of PNSS signaling are essentially the same regardless of the exact form of angle modulating the carrier.

Some of the principal advantages of the spread spectrum approach discussed and spread spectrum techniques in general are their operation in the presence of strong interfering signals such as deliberate jamming and other users. In addition, the signals are not easily detectable because they tend to blend into the background noise. Another advantage is that the spread spectrum signals can aid in multipath rejection. It is relatively easy to also incorporate addressing into a spread spectrum system. Historically, one principal disadvantage has been the period of time required for synchronization. Excessive synchronization time is particularly inconvenient in a dynamic interactive type of environment. Rapid advances in technology have recently uncovered some exciting solutions to this problem.

This section of the report begins with a basic discussion of PNSS. The generation and basic properties of pseudorandom sequences are then discussed in the context of PNSS systems. Pseudonoise code synchronization techniques are considered and a quantitative analysis is given developing the processing gain and multiple access capabilities of PN spectrum spreading over a linear channel.

2.2 PSEUDONOISE (DIRECT SEQUENCE) SPREAD SPECTRUM

Pseudonoise (PN), sometimes called direct sequence, is a well known and widely used spread spectrum signaling method. The basic form of a PN signal is that produced by a pseudorandomly PSK modulated carrier. In this modulation, each bit of information is data modulated (eg, ± 1 in binary modulation) upon a sequence of rf carrier chips whose phases are modulated according to the output of a PN sequence generator. The PN chip rate, R_c is much greater than the data rate. A generalized block diagram of a PN spread spectrum transmitter is shown in figure 2-1. A typical biphase PN signal is shown in figure 2-2. Although PSK is mentioned, the characteristic of PN spread spectrum can be achieved by other pseudorandomly angle-modulated rf carriers. Fundamental to the PN modulation is the concept of bandwidth spreading (the transmission of signals whose rf bandwidth is much greater than the message bandwidth). The processing gain of a correlation receiver is equal to TW, where T is the information bit time and W is the spread spectrum bandwidth.
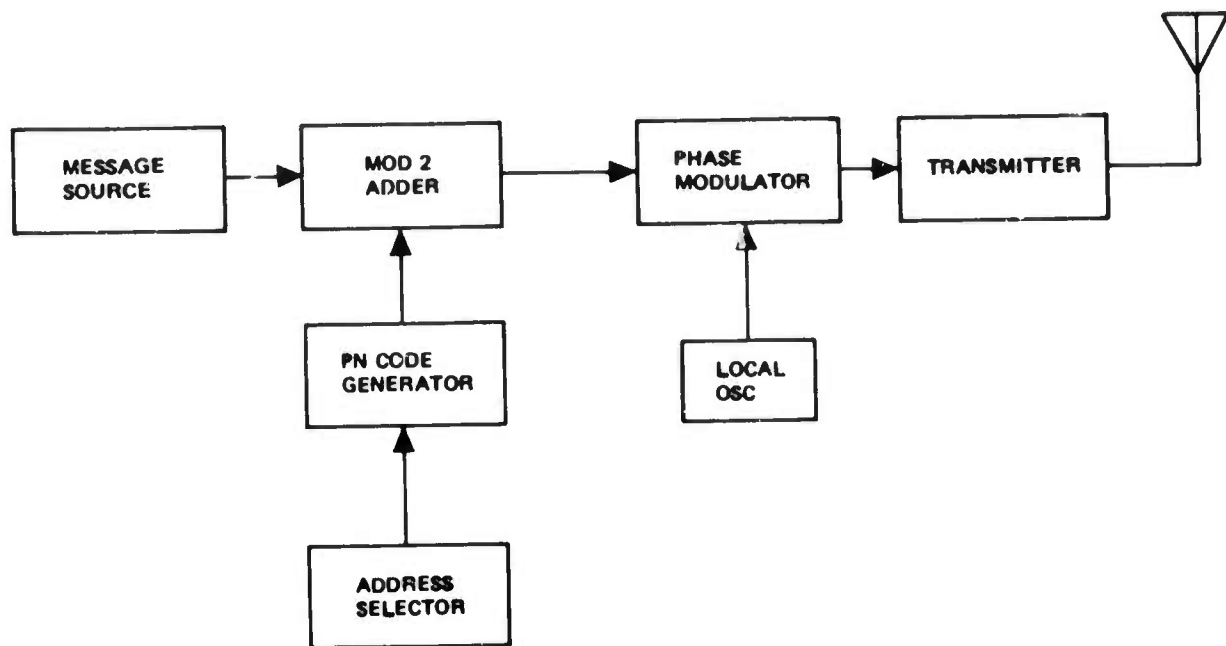
Figure 2-1.   PN Spread Spectrum Transmitter Functional Block Diagram.

Figures 2-3(a), (b), and (c) illustrate the spectrum of a PN modulated signal. The original message spectrum is a narrow spectrum around a carrier frequency, with a main lobe bandwidth (null to null) of 2R for PSK, where R = 1/T is the data rate, as shown in figure 2-3(b).   Since the PN sequence resembles very closely a pure random sequence, the PN modulated signal basically occupies the same bandwidth as that of one rf chip. Hence, the spectrum of the PN modulated signal has a main lobe bandwidth (null to null) of R_c, where R_c is the chip rate of PN modulation; and has side lobes of null-to-null bandwidths equal to the chip rate, as shown in figure 2-3(c). In fact, the power spectrum of the PN signal with PN code period K at chip rate R_c has an envelope of the form

$S/K [\sin (\pi f/R_c) / (\pi f/R_c)]^2$ for PSK, as shown in figure 2-5, where S is the carrier power.

Thus, the total available rf power S is spread over a wideband, its bandwidth spread is directly proportional to the chip rate. The power level at each harmonic is at least reduced by the factor 1/K from the total carrier power, for PN codes with period K. For example, if the PN chip rate is 10 MHz, the spectrum will have a main lobe with 20 MHz bandwidth, and side lobes with 10 MHz bandwidths. If PN codes of period 127 are used, the power spectrum density will be at least 21 dB below the total carrier power at every harmonic over a wideband. Thus, a wideband, low-power density signal that has statistical properties similar to noise is the result. Because of this, PN spread spectrum signals will have little effect on narrowband receivers except for certain near-far relationships. For this system, a casual listener is denied access to the baseband information since it can be recovered from the wideband signal only through correlation with a stored reference sequence in the receiver which is an exact replica of the original encoding sequence. Moreover, substantial processing gain against narrowband jamming can be achieved through band spreading. For example, at data rate of 10 kHz and spread bandwidth of 10 MHz, the
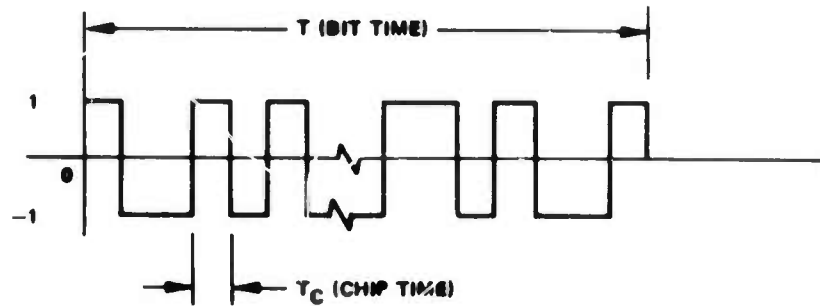
(a) A Typical PN Sequence
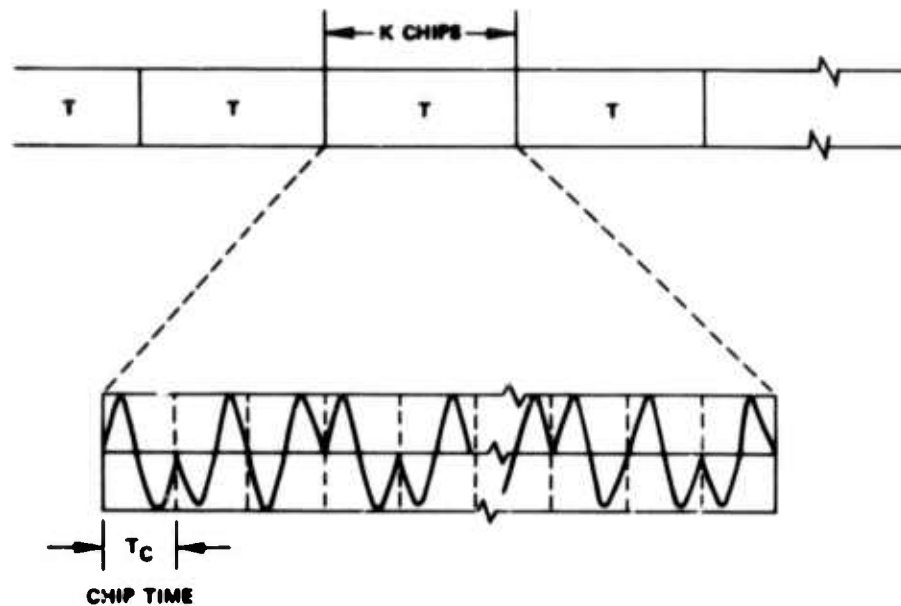
$$S(t) = \pm \sum_{k=1}^{K} P_k(t) \cos(W_C t \pm \Theta_K)$$

$$P_k(t) = \begin{cases} 1 & (k-1)\, T_C < t < k\, T_c \\ 0 & \text{OTHERWISE} \end{cases}$$

$$\Theta_K = \begin{cases} 0 \\ \pi \end{cases} \text{PN SEQ.}$$

(b) Constant Envelope Biphase PN Signal Format

Figure 2-2.   Typical Biphase PN Signal.

Figure 2-3. Spectrum of PNSS Signal in Transmitter/Receiver Processes.

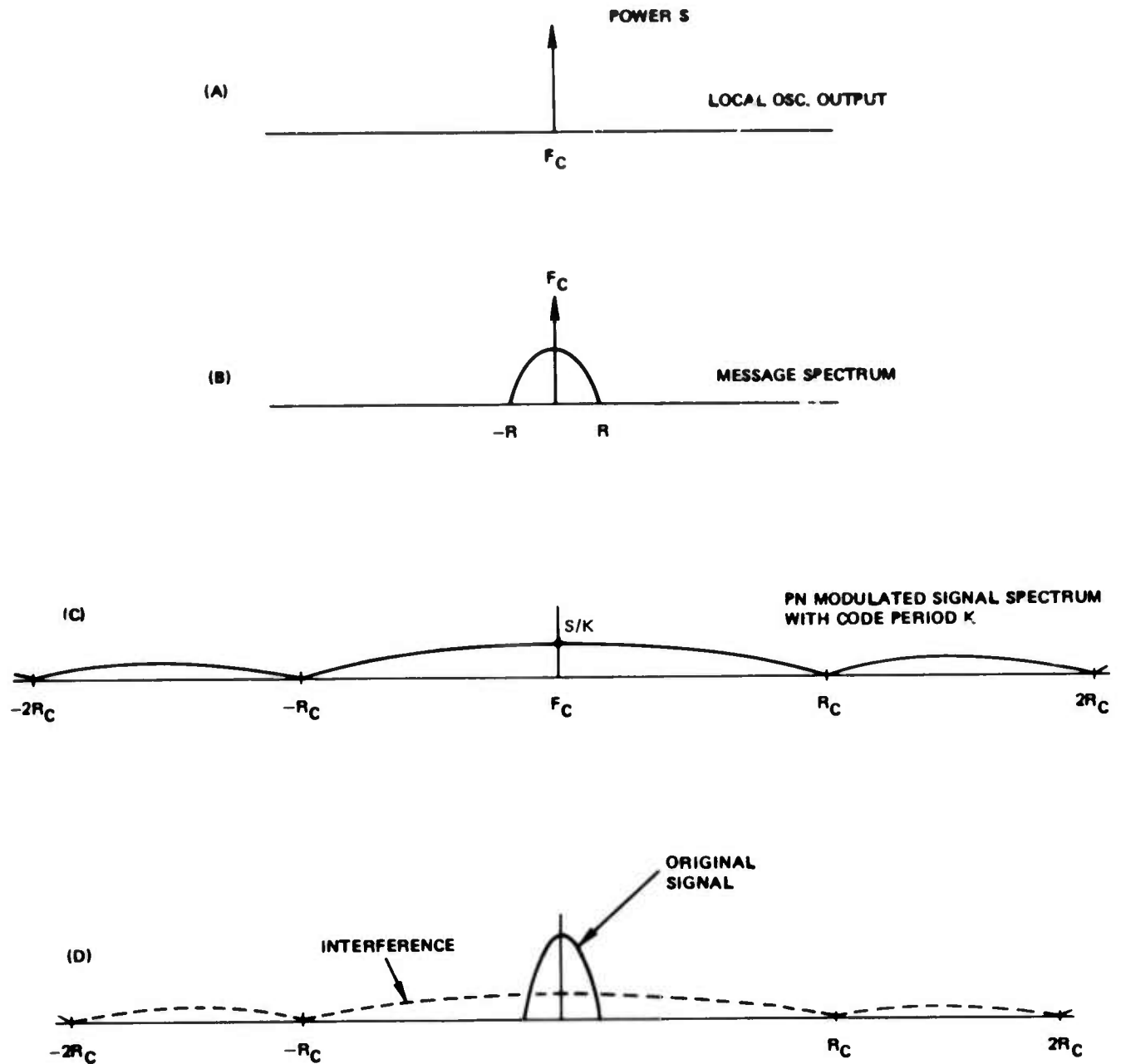AJ processing gain will be 30 dB. For this case, the narrowband interference can be 20 dB above the transmitted signal level, and at the output of the demodulator one obtains a signal-to-noise ratio of about 10 dB.

Figure 2-4 shows a block diagram of a typical PNSS receiver. The incoming PN signal is multiplied by a PN modulated carrier that has the same code as the incoming PN sequence. When acquisition has been obtained, the PN signal carrier is aligned in time to within one chip of the reference PN sequence. The if. output is integrated and dumped. In other words, a correlation is performed for each bit of data with the known PSK/PN sequence. The message is decoded according to the correlation. A+1 will be decoded if the correlation is positive, otherwise a -1 will be decoded. The desired signal lines up with the reference PN code; thus, after multiplying with its own replica (or negative replica), the PN modulation is removed, leaving the baseband information. In frequency domain language, the product of the desired signal and the local reference has a collapsed spectrum equaling that of the original message modulation. The product of the reference signal (itself wideband) and narrowband jammer (CW jammer) will have a wide power spectrum, spreading the jammer power over a wide band. Similarly, the products of the reference signal and other wideband interferences (including noise and other uncorrelated PN modulated signals due to other users in a multiple access operation—the latter resembles very closely wideband noise) are also spread over a wide band. The resulting spectrum of the product of incoming signal and reference is shown in figure 2-3(d). The integrate and dump filter operating over bit time T is a narrowband filter of noise bandwidth 1/T. At the output of the integrate and dump filter only 1/T of the total wideband interference power spectrum bandwidth W appears as the noise power, giving rise to the factor TW as the processing gain against narrowband jammer and uncorrelated PN signals. Thus, AJ and multiple access capabilities are achieved.

2.3 PSEUDORANDOM SEQUENCES

In this section the generation and basic properties of pseudorandom sequences will be discussed. See figure 2-5 for a functional block diagram of the 10-MHz Band Spread, 127 Period PN Signal Generation. PN sequences are periodic binary sequences whose statistical properties resemble pure random sequences. Yet they are deterministic, ie, predictable. The following properties define a periodic binary sequence to be PN:

a. In each period of the sequence the number of 1's differs from the number of 0's by, at most, 1.

b. Among the runs of 1's and 0's in each period, one-half the runs of each kind are of length 1, one-fourth of each kind are of length 2, one-eighth are of length 3, and so on as long as these fractions give a meaningful number of runs.

c. The autocorrelation function of the binary sequence must be as illustrated in figure 2-6(b). In other words, the number of agreements subtracted from the number of disagreements (when a period of the sequence is compared to a cyclic shift of itself) should equal to the period K if the number of shifts is zero, and equal to -1 if otherwise.

As compared to a pure random sequence, whose autocorrelation function is shown in figure 2-6(a), the main difference lies in the periodic nature of the PN sequence as opposed
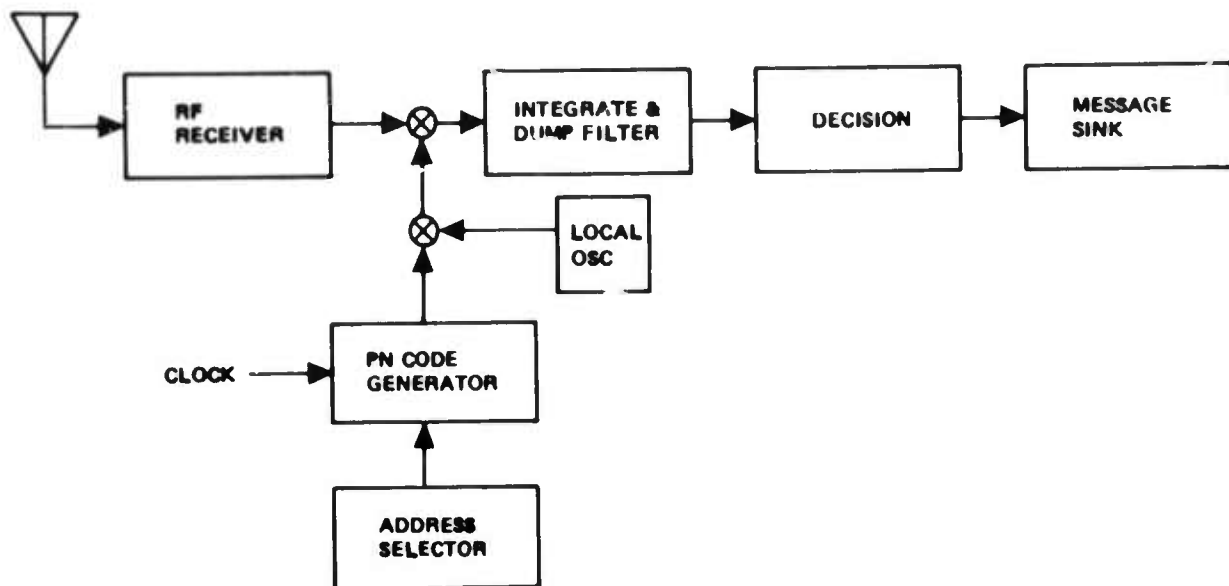
Figure 2-4.   PN Spread Spectrum Receiver Functional Block Diagram.

to the nonperiodic nature of a pure random sequence. The power spectrum of a PN modulated signal, given by the Fourier transform of the normalized autocorrelation function, is then equal to the discrete spectrum,

$$ S(f) = \frac{1}{K^2} \delta(f) + \sum_{\substack{n=-\infty \\ n \neq 0}}^{\infty} \frac{K+1}{K^2} \left[\frac{\sin \pi f/R_c}{\pi f/R_c} \right]^2 \delta\left(f - \frac{n}{KT_c} \right) $$

where K is the period of the PN sequence, T_c is the PN chip time, and $R_c = 1/T_c$ is the chip rate. When K is large, this spectrum is a line spectrum at multiples of $1/KT_c$ with an envelope given by $1/K$ $[\sin \pi f/R_c / \pi f/R_c]^2$, as shown in figure 2-7.   Thus, the spectrum occupancy of a PN spread spectrum signal is exactly known.

It has been known for some time that maximum length linear shift sequences are pseudorandom. Generation of these sequences can be achieved by linear feedback shift registers, a block diagram of which is shown in figure 2-5. Binary sequences generated by linear feedback shift registers depend upon the feedback connections. An n-stage linear shift register may be represented algebraically by a polynomial with binary coefficients that are added and multiplied modulo 2.   The coefficient of the X^k term of the polynomial representing the shift register is 1 or 0, depending on whether or not the feedback tap

$$f(X) = 1 + X^2 + X^3 + X^5$$
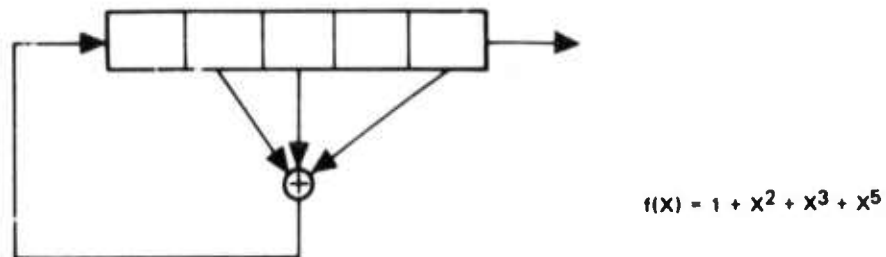
(a) A Five Stage Register and
     Its Polynomial Representation
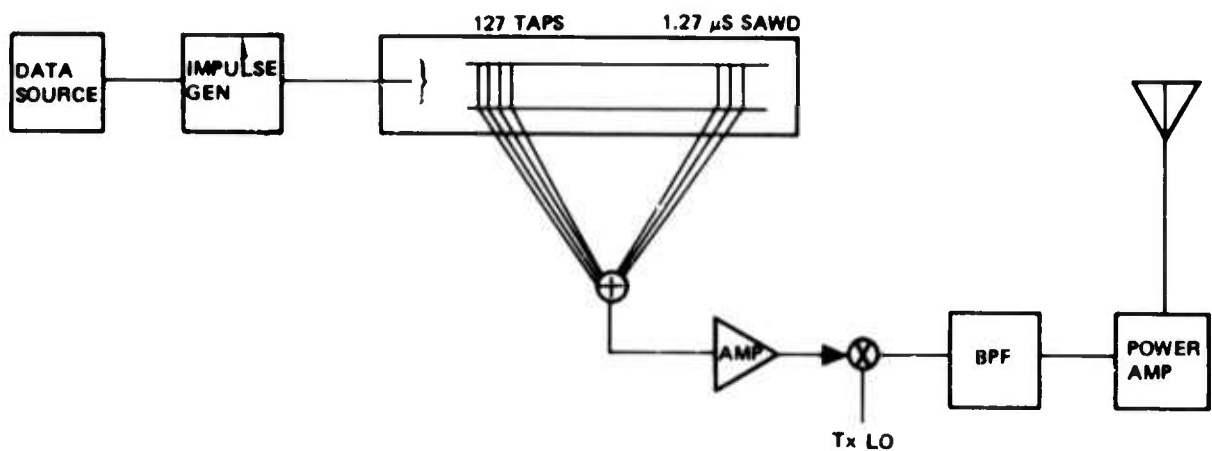
(b) Functional Block Diagram for 10-MHz Band Spread,
     127 Period PN Signal Generation Using
     Surface Acoustic Wave Device (SAWD)

Figure 2-5.   10-MHz Band Spread, 127 Period PN Signal
              Generation Functional Block Diagram.

$$R(t) = \begin{cases} 1 - \dfrac{|t|}{T_C} & |t| < T_C \\ 0 & \text{OTHERWISE} \end{cases}$$
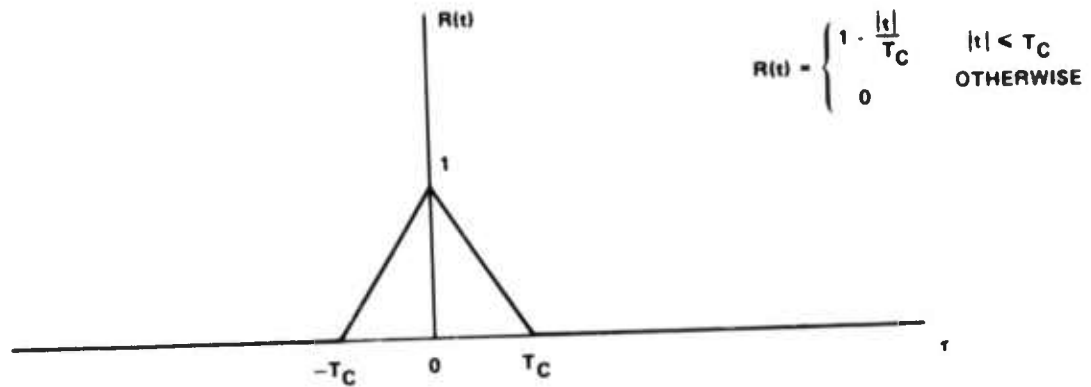
(a) Autocorrelation Function of
a Purely Random Sequence
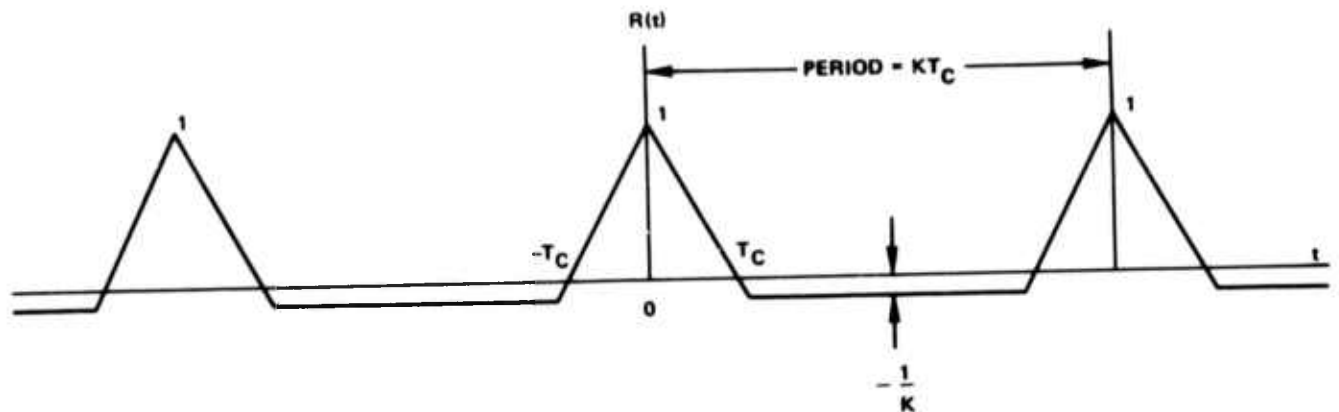
$$\text{ONE PERIOD: } R(\tau) = \begin{cases} 1 - \left(\dfrac{K+1}{K}\right)\dfrac{|\tau|}{T_C} & |\tau| < T_C \\ -\dfrac{1}{K} & |\tau| > T_C \end{cases}$$

(b) Autocorrelation Function of a PN Sequence

Figure 2-6. Autocorrelation Function.

2-8

$$S(f)$$
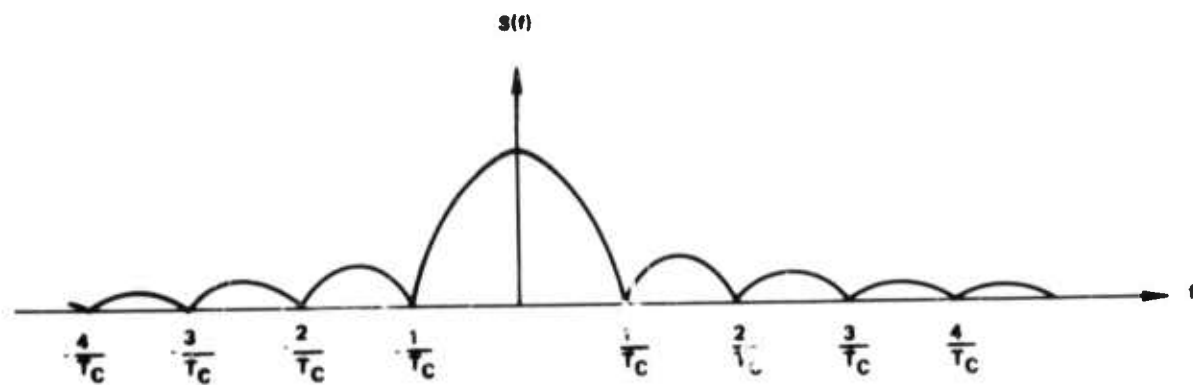
$$S(f) = T_C \left(\frac{\sin \pi f T_C}{\pi f T_C} \right)^2$$

(a) Power Spectrum of a Purely
Random Sequence

$$S(f)$$

←→ SPACING AT $\frac{1}{KT_C}$
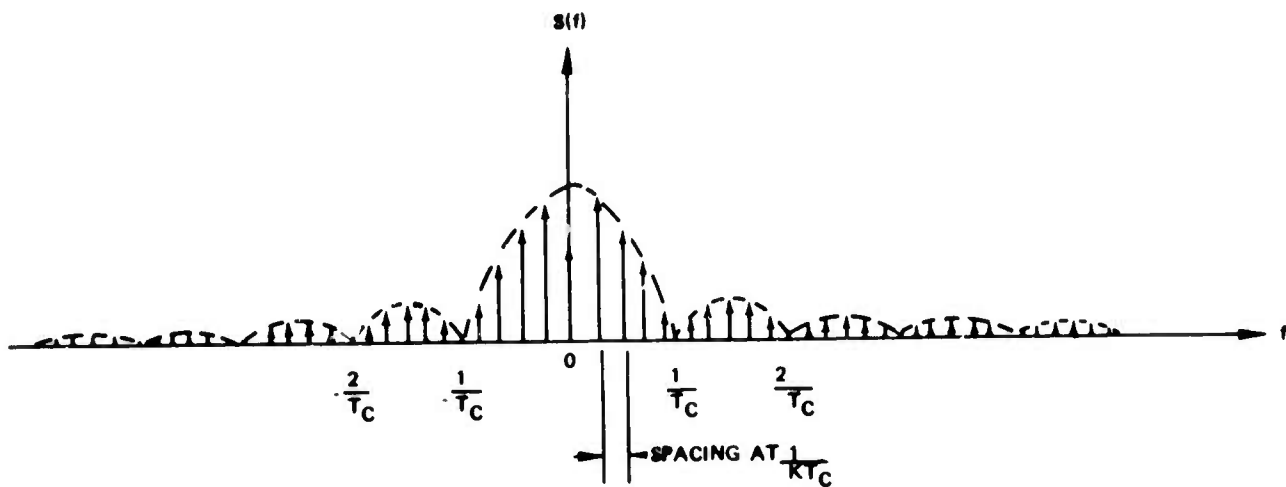
$$S(f) = \frac{1}{K^2} \delta(f) + \sum_{\substack{n=-\infty \\ n \neq 0}}^{\infty} \frac{K+1}{K^2} \left(\frac{\sin \pi f T_C}{\pi f T_C} \right)^2 \delta \left(f - \frac{n}{KT_C} \right)$$

(b) Power Spectrum of a PN Sequence
with Chip Time T_c Period KT_c

Figure 2-7.   Power Spectrum Sequence.

to the kth stage is or is not connected. A five-stage linear shift register and its representing polynomial are shown in figure 2-8. A maximal sequence is a sequence generated by linear shift registers, whose period K is equal to 2^n-1, where n is equal to the number of stages in the shift register. The necessary and sufficient condition on the feedback connections of an n-stage shift register for maximal sequences is that the polynomial representing the shift register is primitive; ie, it divides $1 + X^{2^n-1}$ but no polynomial of the form $1 + X^P$ for $P < 2^n-1$. The number of distinct maximal length sequences generated by an n-stage shift register is $\phi(2^n-1)/n$, where $\phi(K)$ is the number of positive integers less than K and relatively prime to K. For example, a five-stage register will have $\phi(2^5-1)/5 = 6$ primitive polynomials, each generating a maximal sequence of period $2^5-1 = 31$.

Generation of a PN/PSK signal can also be achieved using a surface acoustic wave device, as shown in figure 2-6(b). In this case, no shift registers are necessary. A period of the PN sequence is preprogrammed in the SAWD; input pulses at bit times with data modulation to the SAWD will generate desired PN signals for successive information bits as they arrive.

2.4 PN CODE CROSSCORRELATION AND COEXISTENCE

When correlation is performed between the received signal and a replica reference PN signal at the receiver, the output will be a sum of the following correlations.

a. Correlation between desired signal and reference.

b. Correlation between reference signal and other undesired PN signals sent by coexisting terminals in the same common band.

c. Correlation between reference signal and noise.

d. Correlation between reference signal and narrowband interference (jamming).

When synchronization is obtained, a. will be directly proportional to the energy of the desired signal in one bit of data. For zero mean noise and jamming, c. and d. will both be zero on an average and their variances will directly influence performance; ie, probability of bit error. However, the term b. above will be determined basically by the crosscorrelation between the receiver PN code and that of other undesired transmitters.

If the same PN codes are used among different transmitters, then this correlation will be either -1 or K (K = period of the PN code) for continuous code, depending on whether or not the undesired signal is lined up in time with the desired signal to which the receiver timing is synchronized. Thus, coexistence performance may be tremendously degraded in this case when undesired signals line up in time accidentally with the desired signal.

In most multiple-access operations, different PN codes will be used for different transmitters. It would be ideal if the codes could be designed to be orthogonal between different users pairs. This would require that all the users be synchronized with a centralized control. One example would be where all the transmissions are directed through a single satellite repeater. Since the Packet Radio Network utilizes a distributed control philosophy, such orthoganality between different user pairs is not possible.

$$F(X) = 1 + X + X^5 + X^6 + X^7$$

MAX CROSS CORRELATION = 41

$$F(X) = 1 + X + X^2 + X^7$$
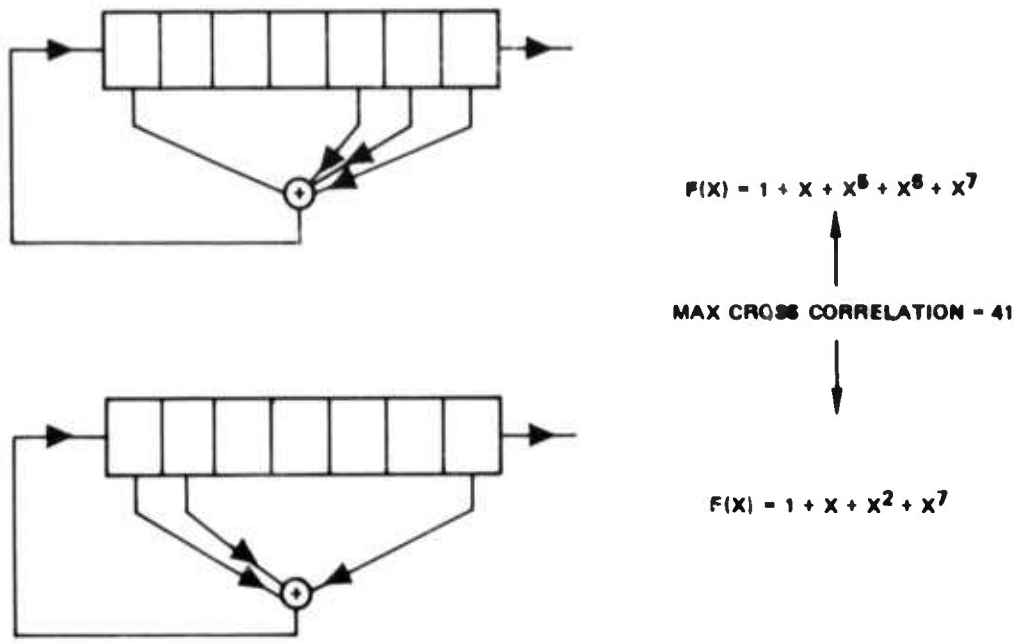
CROSS CORRELATION VALUE	-41	-17	-9	-1	7	15	23
FREQUENCY	1	14	28	36	28	14	7

(a) Two Maximal Length Sequence Generators
and Their Crosscorrelation Values

$$F(X) = 1 + X^2 + X^6 + X^8 + X^{11} + X^{12} + X^{14}$$
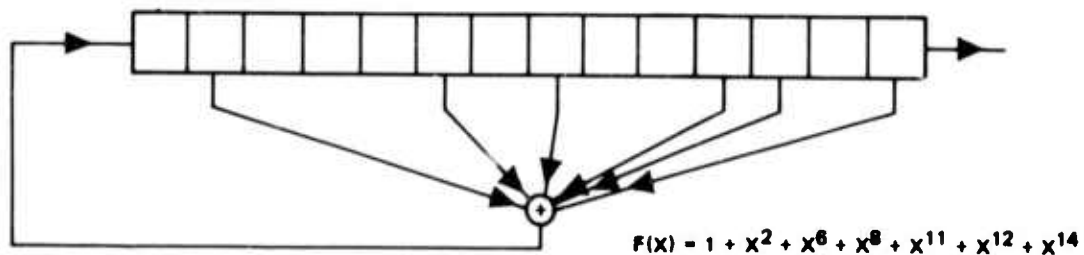
(b) Generators for 129 Distinct Non-Maximal (Gold) Codes
with Periods 127 and Maximum Crosscorrelation 17

Figure 2-8.   Five-Stage Linear Shift Register and Its Representing Polynomial.

More critical than the degradation in signal detection performance is synchronization. The ideal autocorrelation property of a PN code is used for synchronization (see paragraph 2.5). However, when crosscorrelation between different PN codes is large, the receiver bit sync loop may lock onto the crosscorrelation peaks between local reference and undesired PN signals rather than onto the autocorrelation peaks of its own communication link, thus failing to acquire and maintain synchronization. Therefore, the successful use of PNSS systems in multiplexing applications depends upon the construction of large families of encoding sequences with uniformly low crosscorrelation values.

One obvious way to construct these codes is by exhaustive search, however, a deterministic construction algorithm has also been discovered by Gold [1]. Gold's approach is to construct families of non-maximal sequences whose crosscorrelation functions are uniformly small, and whose autocorrelation functions are not two-valued, but nevertheless, the out-of-phase autocorrelation functions are small and have the same bound as the crosscorrelation functions. Gold showed that there are "preferred pairs" of maximal sequences of period $K = 2^n - 1$, where n is the number of shift register stages, whose crosscorrelation function is uniformly bounded by:

$$K|R(\tau)| < 2^{\frac{n+1}{2}} + 1 \qquad \text{for odd n}$$

$$K|R(\tau)| < 2^{\frac{n+2}{2}} + 1 \qquad \text{for even n}$$

For large n, this bound is approximately equal to:

$$K|R(\tau)| < 2\sqrt{2^n - 1} = 2\sqrt{K}$$

Gold has given an algorithm to construct these two preferred pairs of maximal sequences. Let $f_1(X)$, $f_2(X)$ denote the primitive polynomials of these two shift registers. Gold showed that a linear feedback shift register corresponding to the product polynomial $f_1(X) \cdot f_2(X)$ will generate $2^n + 1$ different (non-maximal) sequences each of period $2^n - 1$ and such that the crosscorrelation function of any pair of such sequences are uniformly bounded by $2^{(n+2/2)} + 1$. Their out-of-phase autocorrelation function has the same uniformly small bound.

To illustrate this construction we consider the case n = 7. In other words, we want to construct a family of sequences of periods $2^7 - 1 = 127$, whose pairwise crosscorrelation is uniformly bounded by $2^{(n+1/2)} + 1 = 17$ in magnitude (normalized value $17/127 \simeq 0.134$). This is compared to the maximum autocorrelation value of 127 (normalized value 1). For a 7-stage shift register, there are $\phi(2^7 - 1)/7 = 126/7 = 18$ distinct maximal sequences. It is known that the mutual crosscorrelation function among pairs can be as high as 41 (see figure 2-8 for two maximal sequences in 18 that have this high crosscorrelation). Using Gold's algorithm, one can pick two preferred maximal sequences among the 18 whose crosscorrelation function is bounded by 17. They have the following primitive polynomials:

$$f_1(X) = 1 + X + X^2 + X^3 + X^7$$

$$f_2(X) = 1 + X + X^2 + X^3 + X^4 + X^5 + X^7$$

[1]References are provided at the end of the section.

Then the product polynomial, corresponding to a 14-stage shift register,

$$f_1(X) \cdot f_2(X) = 1 + X^2 + X^6 + X^8 + X^{11} + X^{12} + X^{14}$$

according to Gold's proof, will generate 129 different non-maximal sequences of period 127. The crosscorrelation function of any pair of such sequences will be bounded by 17.

It is of interest to compare Gold's upper bound to the crosscorrelation of purely random binary sequences. For sequences of length 127, the variance of their crosscorrelation is $\sqrt{127}$ = 11.2 (the mean is zero). Thus, Gold's code has crosscorrelation with magnitudes less than the 2σ point, but greater than the 1σ point of the crosscorrelation function between purely random sequences.

2.5 SYNCHRONIZATION CONSIDERATIONS

Since the receiver must have an exactly matching replica of the transmitted PN signal to perform correlation detection, the receiver's copy of the PN code must be in very close time synchronization with the desired transmitted wave. In the case of PNSS, this means that time synchronization must be achieved to within fractions of a PN chip. For example, if a 10-MHz spread spectrum bandwidth is used, the receiver local key stream generator must be locked well within 0.1 microsecond of the epoch of the received signals. Thus, the time synchronization requirement presents one of the critical aspects of PNSS.

For coherent detection of the signal, frequency and phase lock are required in addition to PN code and chip timing alignment. Frequency and phase lock may be achieved through the use of Costas phase-lock loops, or the phase shift may be removed from the incomming signal by squaring a biphase or squaring a quadriphase signal twice. The resulting multiplier signal is then used as a reference in establishing a coherent carrier for demodulation.

PN code alignment and chip timing synchronization makes use of the ideal autocorrelation function of the PN code, mentioned in paragraph 2.3. A classical method of PN signal epoch detection is to sequentially search over all possible clock time positions until a correct position is located, as indicated by an increase in the measured correlation output in magnitude.

A block diagram showing this search implementation is shown in figure 2-9(a). Noncoherent detection is assumed in this implementation.

If the correlation can be performed at wave propagation speed, then the instantaneous value of the correlation between the incoming PN signal and a fixed PN replica at different positions of time/code alignment will be available. Surface acoustic wave devices (SAWD) or charge transfer devices (CTD) can be used to perform this function as shown in figure 2-9(b). Thus, the PN code epoch can be detected in real time, avoiding the long synchronization time required for a serial search.

For a multiple user's environment however, near-field transmitters may have much higher power than the desired signal, causing the out-of-phase crosscorrelation between the reference PN signal and the undesired PN signal to have values very close to (or even higher than) the in-phase correlation value between the desired signal and the reference. This will cause serious problems in PN epoch synchronization. Gold codes mentioned in paragraph 2.4 may improve the situation somewhat, but serious performance degradation may still exist if the undesired coexisting signals are at much higher levels than the desired one.
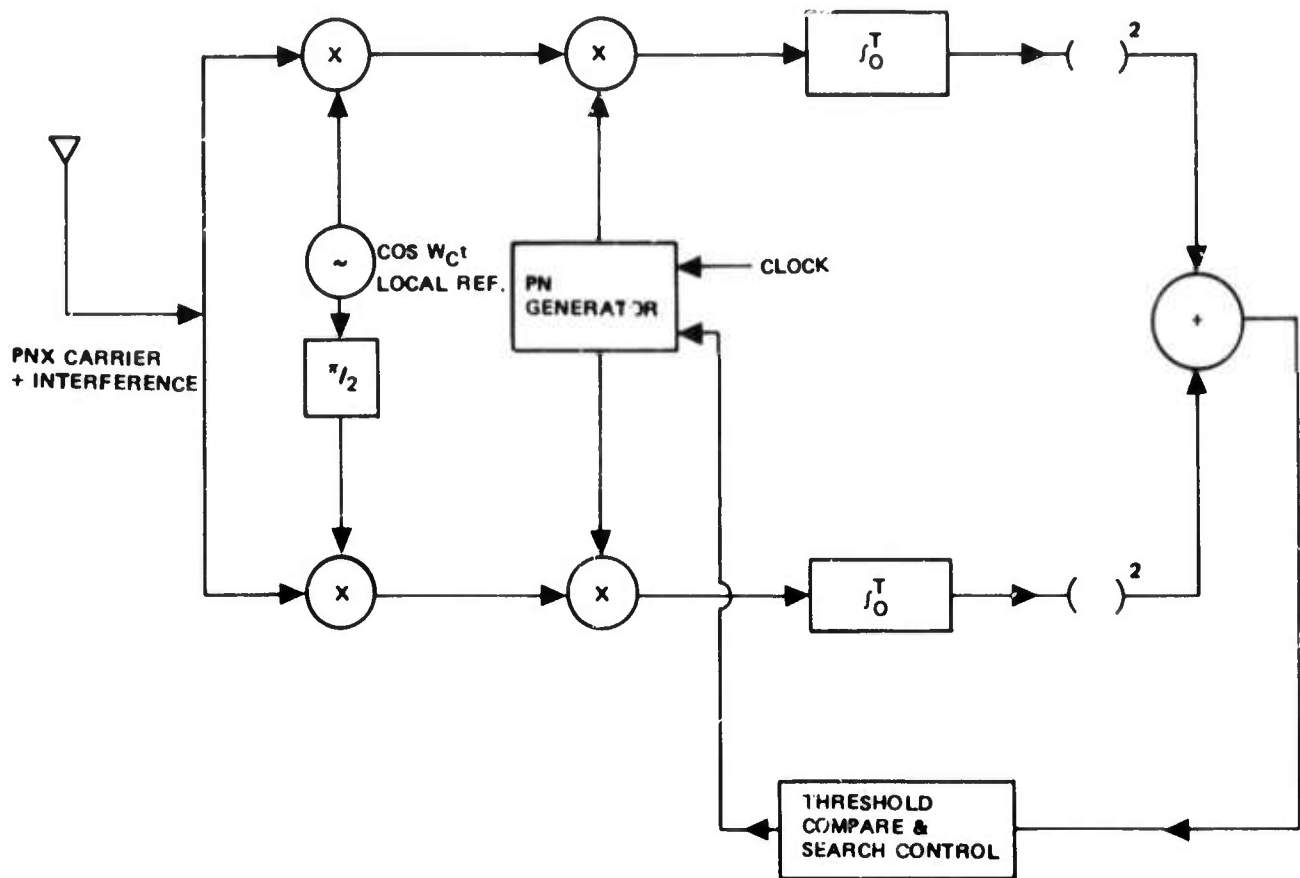
(a) Sequential PN Epoch Detection (Noncoherent)
for PN Code Alignment and Chip Sync
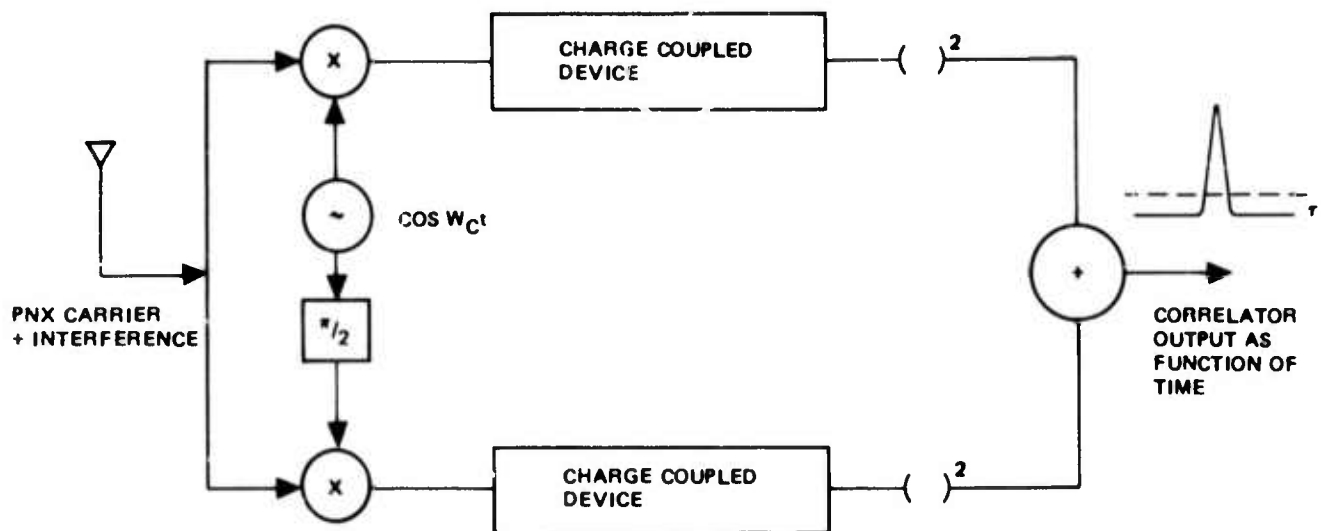
(b) PN Epoch Detection (Noncoherent) in Real–Time
Using Charge Coupled Device

Figure 2-9.   PN Signal Epoch Detection Block Diagram.

Complementary (Golay) codes do provide a two-valued autocorrelation function with zero out-of-phase autocorrelation. Frank codes (polyphase codes) also have zero valued out-of-phase autocorrelation. Crosscorrelation between different pairs of Golay codes is discussed in section 3 of this report.

2.6 PERFORMANCE ANALYSIS OVER A LINEAR CHANNEL

The AJ processing gain and multiple access capabilities of PN spectrum spreading have been explained intuitively in paragraph 2-2. Some quantitative analysis will be given here. For clarity of presentation, most mathematical details are omitted. Also, we shall assume PN/PSK and the channel to be linear. Channels with hard limiting will be discussed.

Consider that a signal bit of duration T is received. The received signal waveform $r(t)$ will be a linear sum of the following:

$$r(t) = s(t) + n(t) + J(t) + C(t)$$

where

$s(t)$ = The desired PN modulated signal with power S

$n(t)$ = Wideband Gaussian noise with one-sided spectral density N_0

$J(t)$ = Interference signal (or jammer) with power J and effective bandwidth B_J

$C(t)$ = Clutter due to other transmitters in the same multiple access band; these are wide bandwidth processes basically uncorrelated with the desired signal.

For simplicity, we neglect $C(t)$ for the moment. For white Gaussian noise, the optimal receiver will be the matched filter. Thus, the receiver performs a correlation between the received signal $r(t)$ and the reference signal, which is an exact replica of the desired PN signal (except for the data modulation ± 1) and is itself wide band. Denoting this reference signal by $S'(t)$, the correlation λ performed over one bit T will be:

$$\lambda = \int_0^T S'(t)\, r(t)\, dt$$

$$= \int_0^T S'(t)\, s(t)\, dt + \int_0^T n(t)\, S'(t)\, dt + \int_0^T J(t)\, S'(t)\, dt \qquad (1)$$

where

$$S'(t) = S(T-t).$$

Since data is decoded according to λ, the statistics λ (which is Gaussian) determines the probability of bit error. In particular, the output signal-to-noise ratio, SNR_0, whose square root is the normalized mean of λ, ie,

$$SNR_0 \triangleq \frac{\bar{\lambda}^2}{\sigma_\lambda^2}$$

where $\bar{\lambda}$ = mean of λ, σ_λ = variance of λ, determines the probability of bit error through the well known error function.

The mean of λ is $\int_0^T S'(t) S(t) \, dt$ since both noise and jammer are zero mean. The variance σ_λ is a sum of variances of the noise and jammer terms. Thus,

$$SNR_0 = \frac{\left[\int_0^T S(t) \, S'(t) \, dt \right]^2}{E\left[\int_0^T n(t) \, S'(t) \, dt \right]^2 + E\left[\int_0^T J(t) \, S'(t) \, dt \right]^2} \tag{2}$$

By Schwartz's inequality, and because $S'(t)$ is directly proportional $S(t)$, we have:

$$SNR_0 = \frac{\int_0^T S^2(t) \, dt \cdot \int_0^T S'^2(t) \, dt}{E\left[\int_0^T n(t) \, S'(t) \, dt \right]^2 + E\left[\int_0^T J(t) \, S'(t) \, dt \right]^2} \tag{3}$$

The power spectrums of the output process obtained from correlating $S'(t)$ with $n(t)$ and $J(t)$ are $|\phi(f)|^2 N_0/2$ and $|\phi(f)|^2 P_J(f)$, respectively, where $\phi(f)$ is the spectrum of the reference signal (ie, the transfer function of the matched filter), N_0 is the one-sided

power spectral density of the noise, and $P_J(f)$ is the power spectral density of the interfering jammer. Since power of a signal is given by integrating its spectral density, and by using the Parseral's theorem, equation (3) can be rewritten as:

$$ SNR_0 = \frac{\int_o^T s^2(t)\ dt}{\frac{N_0}{2} + \frac{\int_{-\infty}^{\infty} |\phi(f)|^2\ P_J(f)\ df}{\int_{-\infty}^{\infty} |\phi(f)|^2\ df}} \tag{4} $$

The spectrum $\phi(f)$, due to PN modulation, has a $(\sin X/X)^2$ envelope with first nulls at R_c (figure 2-7) and effective bandwidth $W = 2R_c$. In general, the jammer bandwidth B_J is $<<W$. A reduction in jammer power is thus seen in equation (4). Also, because of the $(\sin X/X)^2$ shaping of $\phi(f)$, the worst case jammer will be a narrowband jammer centered around carrier frequency. If J is the total jammer power of the jammer, then the resulting SNR_0 is:

$$ SNR_0 = \frac{\int_o^T s^2(t)\ dt}{\frac{N_o}{2} + J/2R_c} \tag{5} $$

The factor 1/2 in the term $J/2R_c$ is due to the phase angle difference between jammer and reference, which is slowly varying between 0 and 2π. Notice this 1/2 factor may be lost in the case of biphase PN when the CW jammer is phase-locked with the reference. In quadriphase (or polyphase PN), however, this factor of 1/2 is always present, which says that biphase PN could have a 3 dB less AJ gain then quadriphase PN under the hypothetical case that phase lock was achieved between jammer and the reference.

If S_1 is the power of the signal to be received, K is the number PN chips for bit, and R_c is the chip rate, then equation (5) can be rewritten as:

$$ SNR_0 = \frac{2K\ S_1}{N_0 R_c + J} \tag{6} $$

showing the number of PN chips per data bit is AJ processing gain.

The case of clutter is very similar to wideband noise. If there are M-1 other active users in the channel, each with different power levels S_m, $m = 2, 3, \cdots, M$; and if $\overline{\rho_m^2}$ is the mean square (normalized) crosscorrelation between the mth user's PN code and the 1st (the desired PN signal), it can be shown that the correlator output SNR_0 will be:

$$SNR_0 = \frac{2K \, S_1}{N_0 R_c + J + \sum_{m=2}^{M} S_m \, K \, \overline{\rho_m^2}} \tag{7}$$

Using Gold's upper bound on PN code crosscorrelations (see paragraph 2.4), $\overline{\rho_m^2}$ will be bounded by:

$$\overline{\rho_m^2} < \frac{1}{K^2} \left(2^{\frac{n+2}{2}} + 1 \right)^2 \approx \frac{4}{K}$$

and equation (7) is reduced to

$$SNR_0 \geq \frac{2K \, S_1}{N_0 R_c + J + \sum_{m=2}^{M} 4 \, S_m} \tag{8}$$

Equation (8) shows that the AJ processing gain is $\sqrt{K}$. Since K is the number of PN chips per data bit, K is equal to the product T (bit time) x W (chip rate) as earlier mentioned.

As an illustration for the foregoing analysis, we consider the following examples:

2.6.1   Example 1.   AJ Capability Analysis

Suppose jammer power is 60 dB above the signal. Neglecting noise and multiple access, this means $10 \log_{10} (SNR_0) = 10 \log 2K - 60$. Requiring SNR_0 to be 13 dB (corresponding to error rate 4×10^{-6}), $\overline{K}$ must be at least 1×10^7. In other words, a PNSS system requires a chip rate in excess of 5 mega chips per data bit to achieve 70 dB AJ processing gain. Of course, this assumes that neither notch filter nor any other nonlinear processing is used.

2.6.2   Example 2.   Multiple Access Analysis

Suppose 127 PN chips are used per data bit.   Assume that each terminal transmits the same power.   Neglecting noise and jamming, $SNR_0 = 2K/4$ (M-1).   If the output SNR_0 is required to be 10 dB, then M = 8.   In other words, no more than 8 simultaneous users should be used. In this analysis Gold's upper bound is used in evaluating the code cross-correlation. Thus, this conclusion may be somewhat conservative. Exact calculations can be performed once the code sets are defined.

2.7   EFFECT OF HARD LIMITING

The effect of hard limited channels will be briefly discussed. Whenever two or more independent signals pass through a hard limiting repeater, the power ratio of any two component signals at the output will generally differ from the power ratio at the input, the change favoring the stronger signal at the expense of the weaker one. The worst case of suppression involves two constant envelope signals, one greater than the other by a factor of 4 or more. The relative output power of the smaller signal is reduced by another factor of 4 (6 dB) below its relative power at the repeater input. CW jamming is one example of this case. In fact, it is known that, for one quadriphase PN user and a tone jammer of power much greater than the desired signal, the presence of a limiter degrades the AJ processing gain predicted in paragraph 2.6 by 6 dB, independently of the jammer phase angle. However, for biphase PN, the jammer phase angle does affect performance. In fact, the biphase PN signal can be significantly suppressed by the tone jammer if the jammer is in phase with the carrier of the desired signal.

In contrast to this worst case (6-dB degradation), if the larger of the two signals can be characterized as a Gaussian process, then the smaller signal is reduced by, at most, 1 dB below its input relative power. When any large constant-envelope signals arrive simultaneously at the repeater input with nearly equal power, the effect is like the Gaussian signal case, so that any one constant envelope signal among them would be suppressed by about 1 dB. In other words, without narrowband jamming, just in the presence of Gaussian noise and clutter, the output SNR_0 will be degraded by about 1 dB from that predicted in paragraph 2.6 if hard limiting occurs in the repeater.

2.8   NEAR-FAR PROBLEM

For a radio network, the number of simultaneous users may be large and some of the users may be located in the vicinity of the receiver, and thus, having much higher power than the desired signal. Coexistence is thus a critical aspect of the PNSS radio network. This problem will be solved if coexisting users use completely orthogonal PN codes. Orthogonality, however, requires that all users be synchronized and is not practical for most radio networks. As paragraph 2.6.2 illustrates, to guarantee an SNR_0 of more than 10 dB for PNSS with 127 PN chips per data bit, no more than eight simultaneous users should be active at the same time. This means that the ratio of total undesired signal power to desired signal power should not be more than 8.2 dB. This figure may be conservative, but it illustrates the drawbacks of a constant envelope PNSS system in terms of near-field coexistence.

Hybrid systems like frequency hopping PN, time hopping PN may improve performance in multiple users' environment.

Requiring each user to transmit signals at lowest level and to increase power only when the repeater failed to acknowledge receiving of the signal may improve performance to some extent. In such a situation, the SNR_0 at the output of receiver correlator is predicted by equation (8).

Another alternative to combat the near-far problem for a pure PNSS system is to send more chips per bit for a distant (low power) user and less chips per bit for closer (higher power) users. An example is given to illustrate this application.

Example:

Consider the case M = 4 users, two of which operate with high power and two of which operate with low power.

$$S_1 = 10$$

$$S_2 = 10$$

$$S_3 = 1$$

$$S_4 = 1$$

Assume noise is negligible and jammer power J = 50. Suppose SNR_0 is required to be 10 for each of the four users, and solve for the minimum allowable K_1, K_2, K_3 and K_4, which indicate the allowable information rates of the four users. From equation (8), the results are

$$K_1 = K_2 = 49$$

$$K_3 = K_4 = 670$$

Since the chip rates are constrained to be equal, the information rates of the two pair of users are in the ratio 670/49 = 13.7. That is, users 1 and 2 may operate at a rate 13.7 times as great as users 3 and 4.

REFERENCE

1. Gold, R., "Optimal Binary Sequences for Spread Spectrum Multiplexing"
   IEEE Trans. on Information Theory, Vol. IT-13, No. 4, October 1967,
   pp 619-621.

REFERENCE

1. Gold, R., "Optimal Binary Sequences for Spread Spectrum Multiplexing"
   IEEE Trans. on Information Theory, Vol. IT-13, No. 4, October 1967,
   pp 619-621.

Code Selection for the Packet Radio Experimental System

3.1 INTRODUCTION

The experimental system is a code spread system where each bit is coded into a pre-determined sequence of chips. The system uses MSK (Minimum Shift Keying) for chip modulation. The MSK chip modulation essentially involves transmitting two sets of biphase modulated chips, staggered by a chip interval, on two quadrature subchannels. The signals on both channels are cosine weighted over every 2-chip interval. Therefore, the resultant transmitted signal is a phase continuous signal despite 1 and 0 transitions of the chip sequences on each subchannel.

Hypothetically, if the two quadrature subchannels would be independent channels, then the chip sequence on either channel could conceivably be selected from any suitable family of codes to give the best autocorrelation peaks with minimum side lobes. Practically, however, the two subchannels, X and Y, are not isolated. Consequently, through individual subchannel matched filters, the MSK signal when correlated at the receiver results in crosscorrelation components between subchannels in addition to the normal autocorrelation components. This is shown by figure 3-1. Therefore, the codes on channels X and Y should have minimum crosscorrelation side lobes in addition to the normal requirements of minimum autocorrelation side lobes. It has to be recognized, however, that since the signals between two channels are staggered by a chip, the baseband crosscorrelation terms do not simply add to the baseband autocorrelation terms. In fact, the cosine weighting over 2-chip interval changes this even further. It has been derived in Packet Radio Temporary Note No. 93 that the magnitude of the receiver matched filter response is given by the following equation:

$$|\text{Envelope Magnitude}| = \sqrt{[R_{XX}(t - T_c) + R_{YY}(t - T_c)]^2 + [R_{YX}(t - 2T_c) - R_{XY}(t)]^2}$$

The above equation suggests that the baseband correlation terms of R_{XX} and R_{YY} are in phase, but R_{YX} lags them by a chip, and R_{XY} leads them by a chip. A computer program, MSKCOR, for the MSK baseband correlation is developed in Packet Radio Temporary Note No. 93. The results of the model described therein, have been confirmed using FFT (Fast Fourier Transform).

It is apparent from the above matched filter response equation that if $R_{XX} + R_{YY}$ go to zero everywhere except for the perfect match, then the problem reduces to one of minimizing the difference of crosscorrelation terms staggered by 2 chips. The Golay complementary pairs of sequences have the property that $R_{XX} + R_{YY}$ equals zero except for zero shift. But, the crosstalk between the two subchannels needs to be investigated for the MSK application.

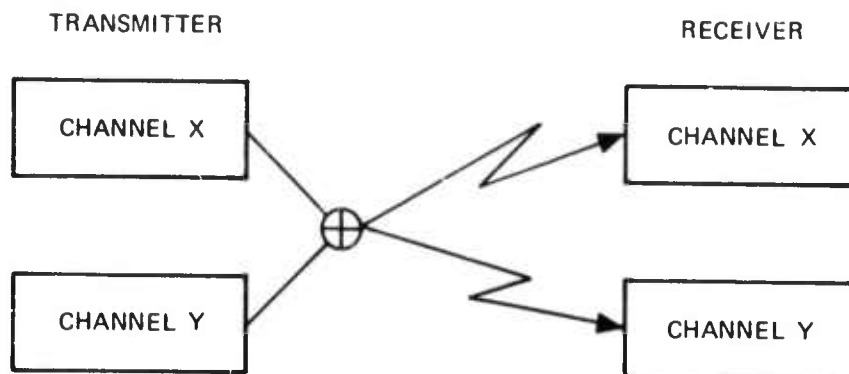TRANSMITTER   RECEIVER

Figure 3-1.   Crosscorrelation Components Between Subchannels.

The packet radio experimental system uses dual data rates of 100 kb/s and 400 kb/s. This imposes additional constraints on any code selection scheme. The codes for the two rates must be different, and the crosscorrelation between codes must be minimum to avoid interference on one data rate detection interfered by transmission of the other data rate signal. The experimental system will have a spread of 128 chips/bit for the 100-kb/s rate, and a spread of 32 chips/bit for the 400-kb/s rate, thereby resulting into 12.8 megachips/s for both data rates. There are 5.25 if. cycles per chip to result in the first stage if. frequency of 67.27 MHz. This is the frequency of the transmit and the receive surface acoustic wave devices (SAWD).

The following paragraphs present the solution to generating the desired length Golay codes, and discuss the code selection process on the basis of minimizing the autocorrelation and the crosscorrelation side lobes. It must be emphasized that because of the baseband model approach developed in Packet Radio Temporary Note No. 93 a viable code optimization scheme has been possible. For example, due to the referenced approach, 5760 possible distinct Golay pairs of 64 length (required for the low data rate 128-chip spread case) are generated and autocorrelated in approximately 45 minutes on the Univac 1108.

Paragraph 3.2 describes the Golay code generation algorithms. Paragraph 3.3 discusses the GOLSEL computer program designed to generate the Golay codes, and to optimize their selection process for the desired autocorrelation characteristics for single data rate systems. Paragraph 3.4 provides the results of code autocorrelation of the 16-length Golay pairs, and the 64-length Golay pairs for the experimental system code investigation. Paragraph 3.5 describes the use of MSKCOR for crosscorrelating of dual data rate codes, and also provides the results of the dual data rate codes crosscorrelation for the experimental system. Paragraphs 3.6 and 3.7 summarize the final code pairs selected along with full details of their side lobe characteristics.

3.2 GOLAY SEQUENCE GENERATION

The basic mechanics of generating sequences of length 2N involve appropriately combining sequences of length N. Begin with the known kernel of length 2 and build up longer sequences with lengths of 4, 8, 16, 23, 64, etc. One conjecture is that for a sequence length of 2^n, there are $n! \, 2^{n-3}$ (n > 2) possible distinct Golay pairs[1]. Based on this result. for a

---
[1]Reference is found at the end of the section.

sequence length of 64, n = 6, and there are 5760 distinct pairs. Similarly, for a length of 16 (applicable for the high data rate 32-chip spread case) there are 48 distinct pairs of sequences.

If X and Y denote complementary sequences subscripted by the desired length, then a particular set of algorithms can be used to generate the predicted number of distinct sequences and their Golay complements. The algorithms are presented in table 3-1.

3.3 CODE SELECTION PROGRAM

A GOLSEL program is written to select a given length code based on certain predefined constraints. The program includes generation of codes based on table 3-1. Figure 3-2 is a representative flow chart of the mechanics of the optimization process.

Basically, as is apparent from figure 3-2 also, the desired code length is called as an input to the program. The length has to be 2^n (where n > 2) for this particular program because the generation is based on a kernel length of 2. The starting code is a pair of length 4 where the code X_4 is 1 1 1 0 and the code Y_4 is 1 1 0 1. Higher length codes are then generated through subroutine GOLGEN by means of algorithms of table 3-1. First, the length 8 pairs are generated. As pointed out in note 5 of the referenced table, the distinct six pairs of length 8 are generated by using algorithms #1-6. These algorithms are referred to as M_1. For example, if $M_1 = 5$, then

$$X_8 = X_4 \underset{1}{} Y_4 = (1\ 1\ 1\ 0)_1(1\ 1\ 0\ 1) = 1\ 1\ 1\ 1\ 1\ 0\ 0\ 1$$

$$Y_8 = X_4 \underset{1}{} \overline{Y}_4 = (1\ 1\ 1\ 0)_1(0\ 0\ 1\ 0) = 1\ 0\ 1\ 0\ 1\ 1\ 0\ 0$$

That is, the code pairs X_4 and Y_4, or X_4 and $\overline{Y}_4$ are simply interleaved.

Further, to obtain the 48 distinct pairs of length 16 for each M_1, algorithms #1-8 must be used. These algorithms are referred to as M_2. For example, if $M_1 = 5$ and $M_2 = 3$, then

$$X_{16} = X_8^* \ \vdots \ Y_8 = (1\ 1\ 1\ 1\ 1\ 0\ 0\ 1)^* \ \vdots \ (1\ 0\ 1\ 0\ 1\ 1\ 0\ 0)$$
$$= 1\ 0\ 0\ 1\ 1\ 1\ 1\ 1\ 1\ 0\ 1\ 0\ 1\ 1\ 0\ 0$$

$$Y_{16} = X_8^* \ \vdots \ \overline{Y}_8 = (1\ 1\ 1\ 1\ 1\ 0\ 0\ 1)^* \ \vdots \ (\overline{1\ 0\ 1\ 0\ 1\ 1\ 0\ 0})$$
$$= 1\ 0\ 0\ 1\ 1\ 1\ 1\ 1\ 0\ 1\ 0\ 1\ 0\ 0\ 1\ 1$$

Although for convenience, the flow chart in figure 3-1 applies to generating and optimizing codes up to length 16, the generation and optimization of higher length codes are an extension of this procedure. It may be noted for further reading that M_3 will refer to algorithm assignments for extending length 16 to length 32, and M_4 will refer to algorithm assignments relating to extension of length from 32 to 64. M_3 can vary from 1 to 10, and M_4 from 1 to 12. Therefore, the maximum number of distinct 64 length Golay pairs is $M_1 M_2 M_3 M_4 = 6.8.10.12 = 5760$.

Table 3-1. Algorithms.

1. $X_{2N} = X_N \mid Y_N$ $\qquad$ $Y_{2N} = X_N \mid \overline{Y}_N$

2. $X_{2N} = Y_N \mid X_N$ $\qquad$ $Y_{2N} = Y_N \mid \overline{X}_N$

3. $X_{2N} = X_N^* \mid Y_N$ $\qquad$ $Y_{2N} = X_N^* \mid \overline{Y}_N$

4. $X_{2N} = Y_N \mid X_N^*$ $\qquad$ $Y_{2N} = Y_N \mid \overline{X_N^*}$

5. $X_{2N} = X_{N\searrow 1} Y_N$ $\qquad$ $Y_{2N} = X_{N\searrow 1} \overline{Y}_N$

6. $X_{2N} = Y_{N\searrow 1} X_N$ $\qquad$ $Y_{2N} = Y_{N\searrow 1} \overline{X}_N$

7. $X_{2N} = X_{N\searrow 2} Y_N$ $\qquad$ $Y_{2N} = X_{N\searrow 2} \overline{Y}_N$

8. $X_{2N} = Y_{N\searrow 2} X_N$ $\qquad$ $Y_{2N} = Y_{N\searrow 2} \overline{X}_N$

9. $X_{2N} = X_{N\searrow 2} Y_N$ $\qquad$ $Y_{2N} = X_{N\searrow 4} \overline{Y}_N$

10. $X_{2N} = Y_{N\searrow 4} X_N$ $\qquad$ $Y_{2N} = Y_{N\searrow 4} \overline{X}_N$

11. $X_{2N} = X_{N\searrow 8} Y_N$ $\qquad$ $Y_{2N} = X_{N\searrow 8} \overline{Y}_N$

12. $X_{2N} = Y_{N\searrow 8} X_N$ $\qquad$ $Y_{2N} = Y_{N\searrow 8} \overline{X}_N$

Notes: 1. $\overline{X}_N$ or $\overline{Y}_N$ imply sequence inverted; i.e., if X_4 is 1 1 1 0, then $\overline{X}_4$ means 0 0 0 1.

2. X_N^* or Y_N^* imply sequence conjugate; i.e., if X_4 is 1 1 1 0, then X_4^* means 0 1 1 1.

3. $X_N \mid Y_N$ imply a union of two sequences. If X_4 is 1 1 1 1 and Y_4 is 0 0 0 0, then $X_N \mid Y_N$ means 1 1 1 1 0 0 0 0.

Table 3-1.   Algorithms (Cont).

Notes: 4. $X_N \diagdown_I \diagup Y_N$ implies interleaving two sequences every I; i. e., if X_4 is 1 1 1 1 and Y_4 is 0 0 0 0, then $X_4 \diagdown_1 \diagup Y_4$ means 1 0 1 0 1 0 1 0, and $X_4 \diagdown_2 \diagup Y_4$ means 1 1 0 0 1 1 0 0 and so on.

5.   To obtain X_4 and Y_4, use algorithm 1.   To obtain the six distinct $X_{8's}$ and $Y_{8's}$, use algorithms 1 through 6.   To obtain the 48 distinct $X_{16's}$ and $Y_{16's}$, use algorithms 1 through 8 to each of the distinct $X_{8's}$ and $Y_{8's}$.   To obtain the 480 distinct $X_{32's}$ and $Y_{32's}$, use algorithms 1 through 10 on each of the distinct $X_{16's}$ and $Y_{16's}$.   To obtain the 5760 distinct $X_{64's}$ and $Y_{64's}$, use algorithms 1 through 12 on each distinct X_{32} and Y_{32}, etc.

It is evident from figure 3-2 that as each code of a desired length is generated, it first goes through the MSKCOR subroutine before the next distinct code is generated. The MSKCOR subroutine uses the MSK correlation model approach described in Packet Radio Temporary Note No. 93.   The correlation process normally involves correlating 2 bits propagating past 1 bit; that is, either CODE followed by CODE can be correlated with the same CODE to give autocorrelation in the sequential mode, or CODE followed by $\overline{\text{CODE}}$ can be correlated with the CODE.   In later presentations, the first mode of correlation will be normally referred to as C C * C and the second mode of correlation will be referred to as C $\overline{\text{C}}$ * C.   The MSKCOR subroutine is preselected for either of the two modes of correlation; that is, C C * C or C $\overline{\text{C}}$ * C.

The code first propagating past the matched filter (or the first bit propagating past the detector SAWDS) results in autocorrelation side lobes which are ignored.   Similarly, the side lobes resulting at the tail end, when the code is not followed by anything, are also ignored. The only relevant side lobes considered are the ones that reflect a normal mode of data detection where each data bit, except for the first and the last, is either followed or preceded by another data bit. The mean, variance, and the peak of the relevant side lobes are written and stored for each distinct pair of M_1 and M_2 for the 16-length Golay

pairs.   The mean, peak, and variance of the next code can be compared for any desired optimization strategy selected.   The present GOLSEL configuration is based on listing mean variance and peak of all codes, and finding the code that gives the minimum peak and the minimum mean.   Equal weighting is given to all of the parameters. In fact, the approach is presented here to demonstrate that the optimization strategy can be predetermined and implemented accordingly; however, the result would be more important for single data rate detector cases since in the case of the multiple data rate detectors the crosscorrelation side lobes also must be considered. A typical output from the GOLSEL program is listed in table 3-2 for reference for the 16-length Golay pairs.

Note that in order to minimize the computer processing time, all of the 5760 codes of length 64 need not be subjected to GOLSEL in either the C C * C or the C $\overline{\text{C}}$ * C mode. Instead, only the C * C correlation needs to be done for all the 5760 codes. A general observation from the C * C, the C C * C, and the C $\overline{\text{C}}$ * C correlations of 16-length pairs
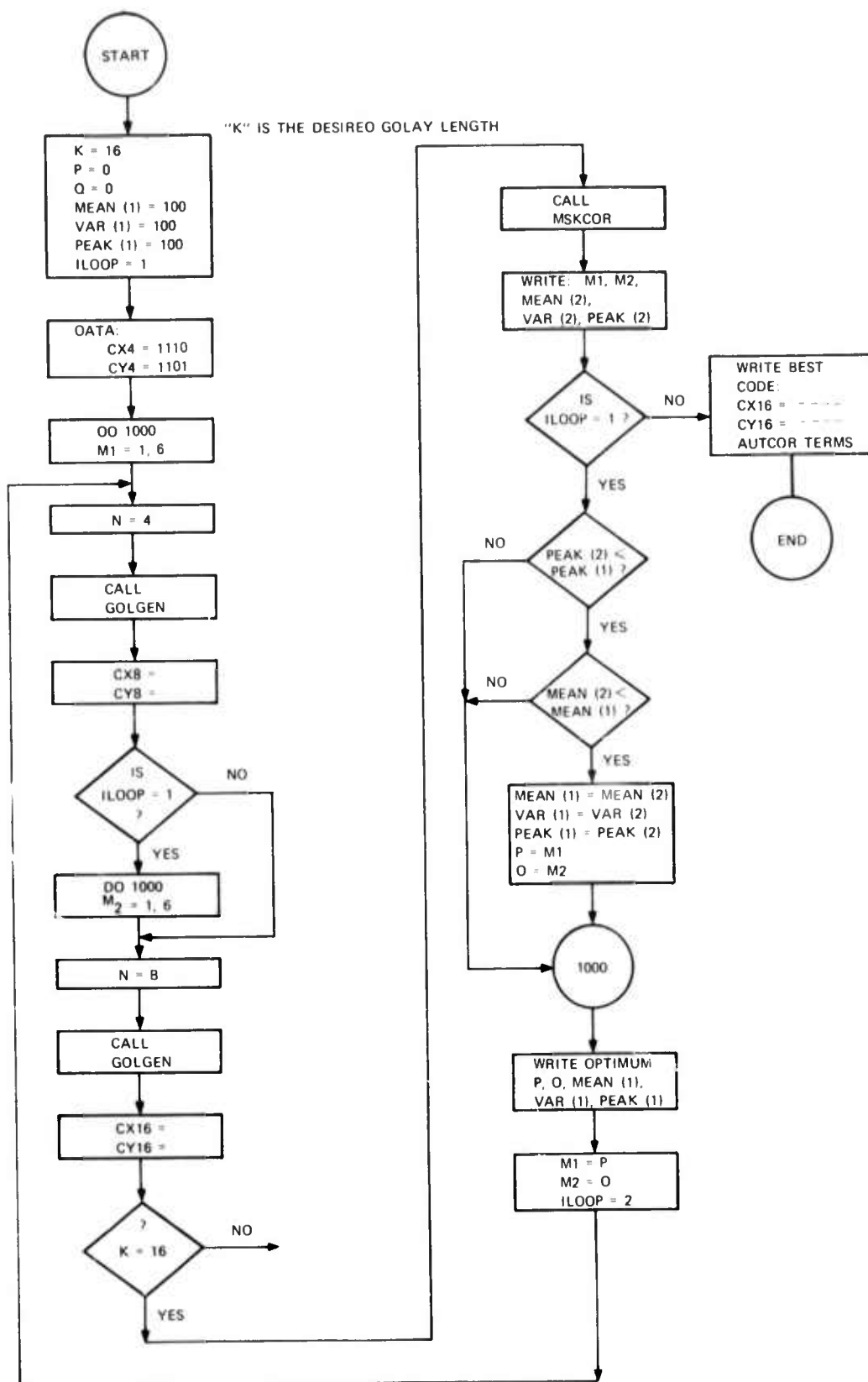
Figure 3-2.   GOLSEL Program Flow Chart.

Table 3-2.   GOLSEL Program Typical Output Listing.

M1	M2	M3	M4	MEAN	VARIANCE	PEAK
1	1			3.31	5.88	8.00
1	2			3.31	5.88	8.00
1	3			2.63	10.57	12.00
1	4			2.63	10.57	12.00
1	5			3.41	10.59	12.00
1	6			1.65	5.32	8.00
1	7			2.44	9.84	12.00
1	8			2.55	7.64	8.00
2	1			3.31	5.48	8.00
2	2			3.31	5.88	8.00
2	3			2.14	10.25	12.00
2	4			2.14	10.25	12.00
2	5			2.44	4.86	8.00
2	6			2.92	12.00	12.00
2	7			2.44	9.84	12.00
2	8			2.55	7.64	8.00
3	1			2.72	9.46	12.00
3	2			2.72	9.46	12.00
3	3			2.33	10.13	12.00
3	4			2.33	10.13	12.00
3	5			2.83	6.72	8.00
3	6			2.53	10.45	12.00
3	7			2.83	6.72	8.00
3	8			2.53	10.45	12.00
4	1			2.53	9.49	12.00
4	2			2.53	9.36	12.00
4	3			2.63	9.36	12.00
4	4			2.63	9.36	12.00
4	5			2.53	6.72	8.00
4	6			2.53	10.45	12.00
5	1			2.83	6.72	8.00
5	2			2.53	10.45	12.00
5	3			2.75	5.74	8.00
5	4			2.25	5.74	8.00
5	5			2.63	5.10	8.00
5	6			2.63	5.10	8.00
5	7			1.76	10.52	12.00
6	8			1.76	10.52	12.00
6	1			2.73	7.36	8.00
6	2			2.73	7.36	8.00
6	3			2.84	7.47	8.00
6	4			2.84	7.47	8.00
6	5			3.11	6.36	8.00
6	6			3.11	6.36	8.00
6	7			2.44	10.80	12.00
6	8			2.44	10.80	12.00
6				3.22	6.14	8.00
6				3.22	6.14	8.00

FOLLOWING IS THE OPTIMUM OF ABOVE

M1	M2	M3	M4	MEAN	VARIANCE	PEAK
1	6			1.95	5.32	8.00
1	6			1.95	5.32	8.00

Table 3-2. GOLSEL Program Typical Output Listing (Cont).

THE FOLLOWING IS THE OPTIMUM PAIR

CODE X

1   1   1   1   0   1   1   0   0   1   1   0   1

CODE Y

1   0   1   0   1   1   0   0   1   0   0   1   0

RXX AUTOCORRELATION

RYY AUTOCORRELATION

RXY CROSS-CORRELATION

RYX CROSS-CORRELATION

RYX-RXY

Table 3-2. GOLSEL Program Typical Output Listing (Cont).

RXX*RYY

ENVELOP MAGNITUDE PEAK TO PEAK

is that the minimum peak side lobes of C * C result into small peak side lobes for C C * C and C $\bar{C}$ * C. Then, the C C * C and the C $\bar{C}$ * C can be performed on a much smaller number of distinct pairs that correspond to minimum peak side lobes for C * C. This time saving approach is utilized for the low data rate (128-chip length or 64-length pairs) codes for the experimental repeater.

3.4 AUTOCORRELATION OF CODES

The C C * C and the C $\bar{C}$ * C autocorrelation results of all of the 16-length and the 64-length codes are summarized in this section. The 16-length code pairs are applicable for the high data rate, and the 64-length code pairs are applicable for the low data rate.

Table 3-3 lists the C C * C and the C $\bar{C}$ * C autocorrelation results of the 16-length high data rate code pairs. As discussed in the earlier paragraph on code generation algorithms, there are a total of 48 distinct Golay code pairs in this length category. M_1 varies from 1 through 6. For each value of M_1, M_2 varies from 1 through 8. Henceforth, the distinct pairs will be referred to as (M_1, M_2). Assuming that a greater weighting is given to minimizing the peak of all side lobes, it is evident from table 3-3 that the following 13 code pairs give the lowest peaks for both C C * C and C $\bar{C}$ * C:

(1, 1), (1, 2), (1, 6), (2, 8), (3, 5), (3, 7), (5, 2), (5, 3), (5, 4), (5, 7), (5, 8), (6, 2), (6, 7).

The above observation corresponds to the minimum peak side lobe value of 8 for C C * C and 6 for C $\bar{C}$ * C. For a system with a single data rate, code selection with minimum mean-variance combination could be taken from the above 13 codes. But, since the experimental repeater uses dual data rates, this decision is subject to the crosscorrelation side lobes between the two data rate codes.

Table 3-4 lists the C C * C and the C $\bar{C}$ * C autocorrelation results for the 64-length low data rate codes. As discussed in the last section, not all of the 5760 codes are subjected to the C C * C and the C $\bar{C}$ * C mode of autocorrelation. Only 41 out of the 5760 codes that result into a minimum peak of 13 in a nonrepetitive code autocorrelation mode (simply C * C) are considered. The C C * C and the C $\bar{C}$ * C autocorrelation results for these 41 codes are summarized in table 3-3. M_1, M_2, M_3, M_4 vary from 1 to a maximum value of 6, 8, 10, 12 respectively. The distinct pairs of this 64-length class are later referred to as (M_1, M_2, M_3, M_4). There are three codes in length 64 that give the minimum value of peak side lobes for the C C * C and the C $\bar{C}$ * C autocorrelation:

(5, 7, 6, 11), (6, 8, 6, 11), (5, 3, 8, 3)

As presented in table 3-4, for each of the above three Golay code pairs of 64 length, the peak for the C C * C is 16, and the peak for the C $\bar{C}$ * C is 18. There are codes with smaller peak values of 14 for the C $\bar{C}$ * C autocorrelation, but they have much higher peaks for the C C * C autocorrelation.

Table 3-3. High Data Rate (Length 32) Autocorrelation.

M1	M2	c c * c MEAN	c c * c VARIANCE	c c * c PEAK	c c̄ * c MEAN	c c̄ * c VARIANCE	c c̄ * c PEAK
1	1	3.31	5.88	8.00	3.02	4.39	6.00
1	2	3.31	5.68	8.00	2.03	4.95	6.00
1	3	2.63	10.57	12.00	3.51	6.93	10.00
1	4	2.63	10.57	12.00	2.24	7.81	6.00
1	5	3.41	10.59	12.00	3.41	8.06	10.00
1	6	1.95	5.32	8.00	2.43	7.88	6.00
1	7	2.44	9.04	12.00	2.62	3.53	10.00
1	0	2.55	7.64	8.00	2.73	6.17	10.00
2	1	3.31	5.48	12.00	2.03	6.10	10.00
2	2	3.31	5.08	12.00	3.51	6.63	10.00
2	3	2.14	10.25	8.00	2.51	6.93	6.00
2	4	2.14	10.25	12.00	2.34	7.41	10.00
2	5	2.44	4.86	12.00	3.01	3.33	10.00
2	6	2.92	12.00	12.00	2.24	6.03	6.00
2	7	2.44	9.84	12.00	2.93	3.62	6.00
2	0	2.72	9.26	12.00	2.51	3.17	10.00
3	1	2.72	9.46	8.00	2.24	10.06	6.00
3	2	2.33	10.13	12.00	2.34	6.69	10.00
3	3	2.33	10.13	8.00	3.51	2.57	6.00
3	4	2.83	10.45	12.00	2.93	2.73	10.00
3	5	2.53	6.72	12.00	2.42	7.10	6.00
3	6	2.03	10.45	12.00	3.40	4.83	6.00
3	7	2.53	6.72	12.00	1.96	5.12	10.00
3	0	2.53	9.49	12.00	2.51	5.39	6.00
4	1	2.63	9.36	8.00	2.24	3.69	10.00
4	2	2.43	9.36	8.00	3.79	6.57	6.00
4	3	2.53	6.72	8.00	2.15	2.57	6.00
4	4	2.63	10.45	12.00	2.82	6.18	6.00
4	5	2.03	6.72	12.00	2.93	3.10	6.00
4	6	2.53	5.74	8.00	1.95	5.93	10.00
4	7	2.25	5.74	8.00	2.44	5.03	6.00
4	0	2.63	5.10	8.00	2.42	6.31	6.00
5	1	2.63	10.52	12.00	3.21	1.44	6.00
5	2	1.76	10.52	8.00	2.74	4.35	10.00
5	3	1.76	7.36	8.00	3.62	3.32	10.00
5	4	2.73	7.36	8.00	3.51	5.02	6.00
5	5	2.04	7.47	8.00	2.74	3.70	6.00
5	6	2.44	7.47	12.00	2.42	5.92	6.00
5	7	3.11	6.36	12.00	2.44	6.69	10.00
5	0	3.11	6.36	8.00	2.84	2.57	10.00
6	1	2.44	10.60	12.00	2.42	5.69	6.00
6	2	2.41	10.60	12.00	2.44	6.72	10.00
6	3	3.22	6.14	8.00	2.84	5.02	6.00
6	4	3.22	6.11	8.00	2.74	3.05	6.00

Table 3-4. Low Data Rate Code (Length 128) Autocorrelation.

M_1	M_2	M_3	M_4	C C • C			c $\bar{c}$ • c		
				Mean	Var	Peak	Mean	Var	Peak
1	8	1	7	5.56	20.64	24	5.13	20.53	22
2	8	2	8	5.53	22.2	20	5.45	16.24	18
3	4	1	8	4.15	31.51	24	5.77	24.3	22
4	6	9	8	5.34	26.66	24	5.67	20.61	18
4	6	10	8	5.34	26.56	24	5.71	20.24	18
5	3	8	7	5.45	24.08	24	5.28	19.67	22
4	8	3	10	5.2	26.05	20	4.49	22.37	22
5	6	3	10	5.11	27.7	24	5.44	25.45	26
6	2	4	9	5.32	25.6	24	4.95	18.41	18
6	3	1	9	4.69	21.27	20	5.78	21.23	22
1	1	1	12	5.09	27.89	24	4.46	22.71	22
2	4	1	12	4.83	20.45	24	5.85	24.26	22
3	4	8	12	5.6	22.65	20	4.79	19.12	14
3	7	5	11	5.37	24.71	20	5.78	23.76	22
3	7	6	11	5.37	24.71	20	5.78	23.76	22
4	3	7	11	5.6	22.65	20	4.84	18.83	14
5	1	5	11	4.93	23.43	20	5.23	17.72	18
5	2	1	12	4.66	20.76	24	5.28	25.36	22
5	6	1	12	5.45	19.66	20	6.04	21.42	26
5	7	6	11	6.09	25.83	16	5.11	22.28	18
6	8	6	11	6.24	24.69	16	5.11	22.28	18
2	2	5	1	5.54	23.74	20	5.55	25.93	22
2	2	6	1	5.41	24.12	20	5.47	26.59	22
3	5	5	1	4.76	20.46	20	5.38	18.7	18
3	5	6	2	4.76	20.46	20	5.38	18.7	18
5	2	7	2	4.85	25.44	16	4.86	19	22
5	5	9	1	4.56	22.28	20	4.74	20.47	22
6	1	4	1	5.56	24.12	20	5.05	20.95	22
6	2	6	1	5.42	25.05	24	5.64	25.1	22
6	3	5	1	5.49	23.35	20	5.51	26.34	22
6	3	6	1	5.29	24.53	20	5.41	26.91	22
3	5	5	4	5.38	26.05	24	5.49	16.18	18
5	3	8	3	4.75	18.32	16	5.36	17.38	18
3	5	1	5	5.36	23.65	24	4.66	15.67	18
3	5	2	6	5.49	23.78	20	4.62	15.74	18
3	5	9	6	5.19	27.43	24	4.51	18.02	18
3	5	10	6	5.19	27.43	24	4.51	18.02	18
4	5	2	6	5.66	22.78	20	5.84	21.7	18
4	5	5	6	5.03	28.75	24	5.6	25.73	22
4	5	6	6	5.03	28.75	24	5.6	25.73	22
6	2	3	6	5.26	22.11	20	5.13	21.2	18

3.5 CROSSCORRELATION OF DUAL DATA RATE CODES

The 13 codes of length 16 and the 3 codes of length 64 which are the preferred candidates based on the minimum peak side lobe criterion, are analyzed for their crosscorrelation properties. However, crosscorrelation between codes is a difficult problem as opposed to the autocorrelation, because it has to take into consideration the different arrival times of the two different rate signals at the receiver. Also, for dual data rates, the cross-correlation has to be performed on two different length codes. The following paragraphs deal with these problems.

3.5.1 Crosscorrelation of High Data Rate Codes into Low Data Rate Codes

This paragraph describes the technique of crosscorrelation for the case when the 32-chip spread high data rate code would interfere with a matched filter at the receiver coded for a low data rate 128-chip spread code; that is, the interference seen by a 64-length Golay pair due to a 16-length Golay pair. It is readily apparent that there is 4 bits worth of high data rate information interfering with the detection of 1 bit worth of low data rate information. To deal with both, the unequal arrival times of the two rate signals and the unequal code lengths under consideration, one of the most effective methods of crosscorrelation, perhaps, is to assume that there always is one of the 16 distinct combinations of 4 bits of short code arriving at the receiver followed by a short C or a $\overline{C}$. This means that a 5-short bit length signal is required. The model MSKCOR program is written to handle correlation of 2 bits long signal with a 1 bit long detector. Since the two long bit length signal is required, the last three short code bits of the signal can be added arbitrarily. Figure 3-3 shows the mechanics of this scheme of crosscorrelation.

As shown in figure 3-3, the crosscorrelation side lobes that would enter consideration are the ones appearing for a short code bit interval immediately following the first full long bit interval; that is, just after the first four short code bits have been correlated without being preceded by any signal. If all the side lobes in this short code bit timeframe just referenced are considered, it is apparent that none of the side lobes that would occur due to the uneven timing between the two rate signals have been ignored. This method gives a true estimate of the peak interfering side lobe; however, how often those peaks would occur is obviously data dependent. For each of the 32 combinations, the side lobe peak, mean and variance values are found. This is used to evaluate the crosscorrelation of the high data rate codes into the low data rate codes.

The results of crosscorrelating the 13 short codes with 3 long codes selected are summarized in table 3-5. A computer output showing all possible crosscorrelation side lobes due to two of the preferred code sets is provided in table 3-6 for reference purposes. The final selection has to be kept pending until the crosscorrelation of the low data rate codes into the high data rate code is analyzed.

3.5.2 Crosscorrelation of Low Data Rate Codes into High Data Rate Codes

The crosscorrelation of the low data rate long codes with the high data rate short codes is relatively simple since the correlator bit length is 32 chip compared to the interfering code bit length of 128 chip. Therefore, the assumption is that the interfering code signal can be C followed by C, or C followed by $\overline{C}$. The process need not be repeated for $\overline{C}$ followed by $\overline{C}$, or $\overline{C}$ followed by C, as the overall results will be identical.
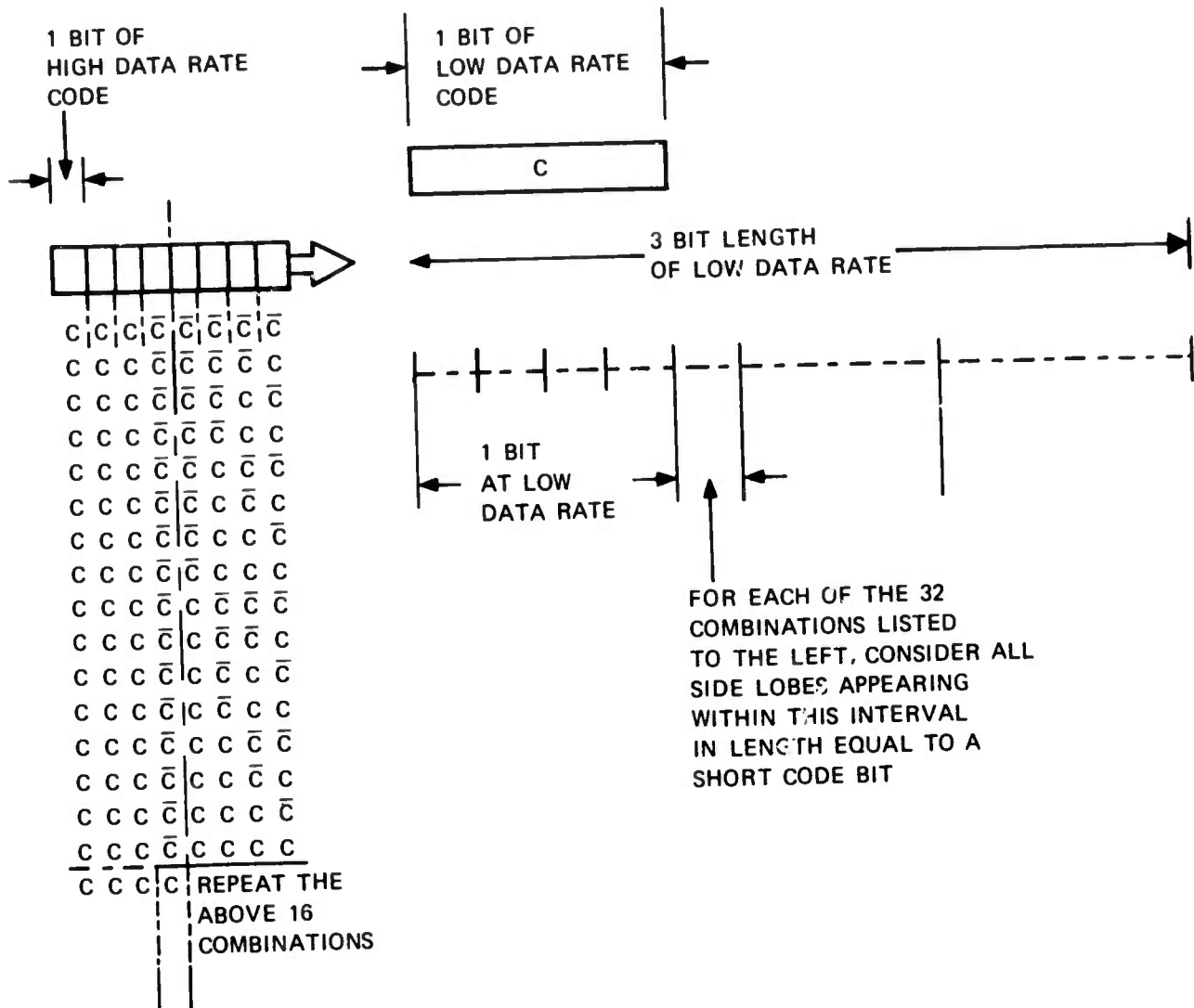
Figure 3-3.   High Data Rate into Low Data Rate Crosscorrelation.

Table 3-5. High Data Rate Code (Length 32) into Low Data Rate Code (Length 128) Crosscorrelation.

16 CODE	64 CODE 5, 3, 8, 3			64 CODE 5, 7, 6, 11			64 CODE 6, 8, 6, 11		
	PEAK	MEAN	PEAKS > 18	PEAK	MEAN	PEAKS > 18	PEAK	MEAN	PEAKS > 18
1, 1	32.2	10.8	132	37.4	9.44	120	33.58	9.421	116
1, 2	34.0	10.3	100	45.1	9.29	118	38.0	9.9	124
1, 6	32.0	10.7	132	36.35	10.2	140	32.4	9.85	138
2, 8	36.5	10.6	110	44.0	9.84	124	36.09	9.68	124
3, 5	33.98	10.4	124	41.9	10.0	124	44.66	10.37	146
3, 7	40.0	10.7	126	34.8	9.4	114	34.02	10.38	178
5, 2	38.2	10.0	120	45.1	8.8	120	39.34	8.8	128
5, 3	44.8	10.57	138	37.4	9.6	122	32.9	9.5	110
5, 4	36.35	9.84	110	42.3	9.0	98	42.3	9.86	146
5, 7	32.07	10.6	122	40.32	10.0	132	33.6	9.68	110
5, 8	32.4	10.35	100	36.0	9.8	144	34.38	9.49	128
6, 2	32.4	10.46	108	34.4	8.55	90	44.00	9.4	122
6, 7	32.6	10.43	136	36.1	9.84	126	36.2	10.45	140

Table 3-6. Length 32 Code (5, 3) into Length 128 Code (6, 8, 6, 11) Crosscorrelation.

CODE 161 5. 31+CODE 641 6. 8. 6.11)

RECEIVED CODE 16 SEQUENCE IS 1 1 1 1 FOLLOWED BY CODBAR OR CODE FOR 1ST AND 2ND OUTPUTS RESPECTIVELY

ENVELOP MAGNITUDE

```
4.14  7.87  16.05  3.24  8.86  10.32  16.05  14.90  5.09  16.31  30.96  16.38  22.15  8.91   6.00
5.09  16.00  2.55  18.71  16.45  7.87   7.64  16.71  5.47   7.64  27.92  32.03  22.00  32.90  10.38
```

ENVELOP MAGNITUDE

```
4.77  9.43  16.20  2.55  9.46  16.20  16.20  9.48  5.09  16.20  17.73  12.95  16.20  7.94   5.00
5.09  6.00  2.55   2.55  9.48  16.20   7.64  8.00  5.09   7.64  16.20   6.00  16.20  17.73  9.48
```

RECEIVED CODE 16 SEQUENCE IS 0 0 0 1 FOLLOWED BY CODBAR OR CODE FOR 1ST AND 2ND OUTPUTS RESPECTIVELY

ENVELOP MAGNITUDE

```
6.45  2.00  1.27  2.00  2.00  1.27  1.27  2.00  2.00  1.27   8.00   7.64  16.00  8.91   10.00
6.30  16.00  5.09  6.52  18.18  5.09  5.09  2.00  2.00  5.09  18.18   8.40  10.32  18.79  7.87
```

ENVELOP MAGNITUDE

```
1.59  4.00  2.55  4.00  1.27  5.09  5.09  8.00  4.00  7.64  20.00  14.00  24.00  10.18   8.00
6.36  12.00  .00  13.04  16.05  5.09  9.48  9.48  13.04  5.09  29.79  32.23  16.00  32.46  10.18
```

RECEIVED CODE 16 SEQUENCE IS 0 0 1 0 FOLLOWED BY CODBAR OR CODE FOR 1ST AND 2ND OUTPUTS RESPECTIVELY

ENVELOP MAGNITUDE

```
.95  .00  .00  .00  .00  .00  .00  .00  .00  .00  .00  .00  .00  .00  .00
.00  .00  .00  .00  .00  .00  .00  .00  .00  .00  .00  .00  .00  .00  .00
```

ENVELOP MAGNITUDE

```
.22  6.00  1.27  2.00  1.27  3.82  6.00  6.00  6.00  6.34  14.00  6.34  6.00  1.27   2.00
.00  5.00  5.00  18.18  11.96  10.32  .00  11.22  11.22  .00  12.54  24.03  6.52  16.00  7.87
```

Table 3-6. Length 32 Code (5, 3) into Length 128 Code (6, 8, 6, 11) Crosscorrelation (Cont).

RECEIVED CODE 16 SEQUENCE IS 0 0 1 1 FOLLOWED BY 0 0 1 1   CODBAR OR CODE FOR 1ST AND 2ND OUTPUTS RESPECTIVELY

ENVELOP MAGNITUDE

RECEIVED CODE 16 SEQUENCE IS 0 1 0 0 FOLLOWED BY 0 1 0 0   CODBAR OR CODE FOR 1ST AND 2ND OUTPUTS RESPECTIVELY

ENVELOP MAGNITUDE

RECEIVED CODE 16 SEQUENCE IS 0 1 0 1 FOLLOWED BY 0 1 0 1   CODBAR OR CODE FOR 1ST AND 2ND OUTPUTS RESPECTIVELY

ENVELOP MAGNITUDE

RECEIVED CODE 16 SEQUENCE IS 0 1 1 0 FOLLOWED BY 0 1 1 0   CODBAR OR CODE FOR 1ST AND 2ND OUTPUTS RESPECTIVELY

ENVELOP MAGNITUDE

RECEIVED CODE 16 SEQUENCE IS 0 1 1 1 FOLLOWED BY 0 1 1 1   CODBAR OR CODE FOR 1ST AND 2ND OUTPUTS RESPECTIVELY

ENVELOP MAGNITUDE

RECEIVED CODE 16 SEQUENCE IS 1 0 0 0 FOLLOWED BY 1 0 0 0   CODBAR OR CODE FOR 1ST AND 2ND OUTPUTS RESPECTIVELY

Table 3-6. Length 32 Code (5, 3) into Length 128 Code (6, 8, 6, 1i) Crosscorrelation (Cont).

ENVELOP MAGNITUDE

```
6.58  20.00   2.55  13.64  17.73  19.43  32.10  15.79  16.79  13.04   2.55   4.00   2.55   4.00
5.00  12.00  10.18  20.00  12.73  20.00   5.09   0.48  16.79  20.64  10.16  13.04   5.09  12.00
```

ENVELOP MAGNITUDE

```
6.05  18.00   1.27  14.90  17.22  16.41  32.00  14.76  16.79   7.67   3.62  18.00   8.91  10.00   3.62   2.00
5.09  14.00   5.09   3.24   4.86  10.32   5.09   6.00  10.16  10.00  10.16  22.15   8.86  10.32  16.79   7.67
```

RECEIVED CODE 16 SEQUENCE IS 1 0 0 1 FOLLOWED BY   CODBAR OR CODE FOR 1ST AND 2ND OUTPUTS RESPECTIVELY

ENVELOP MAGNITUDE

```
.95  11.22  16.05  14.23  24.13  14.07  16.05  10.38  16.05  11.82   9.71   6.00   6.52   3.62   6.00
6.36  14.00  12.73  24.00  15.25  22.00   2.55  14.90  16.05  11.22  14.90  16.79   5.47   2.55  10.00
```

ENVELOP MAGNITUDE

```
.32   9.68  16.20  15.20  24.03  17.49  16.79  10.94  16.05  10.18  11.06  10.22  12.27   5.09   4.00
6.36  16.00   7.64   8.40  10.22  12.27   2.55   4.00   1.27    .00  24.13  10.22   4.74  16.20   6.46
```

RECEIVED CODE 16 SEQUENCE IS 1 0 1 0 FOLLOWED BY   CODBAR OR CODE FOR 1ST AND 2ND OUTPUTS RESPECTIVELY

ENVELOP MAGNITUDE

```
2.85  13.04  16.00  12.27  24.13  13.34  16.00  10.94  16.00  10.94  14.22  11.06  12.27   5.09   4.00
 .00   4.00   7.64  20.16  11.06   4.74   2.55  13.04  16.00  13.04    .62  24.13  12.27  16.20   6.46
```

ENVELOP MAGNITUDE

```
2.23  11.22  16.05  14.23  24.03  16.19  16.45  10.38  16.00  10.38   7.90   4.10   6.52   3.62   6.00
 .00   6.00   2.55   2.00   1.27   6.00   2.55   2.00    .00   2.00   6.00   3.62   6.00   2.55   2.00
```

RECEIVED CODE 16 SEQUENCE IS 1 0 1 1 FOLLOWED BY   CODBAR OR CODE FOR 1ST AND 2ND OUTPUTS RESPECTIVELY

ENVELOP MAGNITUDE

```
2.86  10.38  32.23  14.00  32.10  24.24   3.82  11.22  16.45  15.41  32.63  26.76  16.97  11.22   3.82   2.00
1.27   6.00  10.18  26.12  12.95   6.52   5.09  22.56  17.22   5.47    .00   7.90  24.53  10.16  16.79   5.47
```

ENVELOP MAGNITUDE

```
3.50  10.18  32.40  16.00  32.23  29.79   7.64   6.48  16.45  17.24  32.00  17.24  16.45   6.44   2.55   4.00
1.27   6.00   5.09   4.00   1.27   4.00   5.09  12.00   6.36   6.00    .00   6.00   6.36  12.00   5.09   4.00
```

RECEIVED CODE 16 SEQUENCE IS 1 1 0 0 FOLLOWED BY   CODBAR OR CODE FOR 1ST AND 2ND OUTPUTS RESPECTIVELY

ENVELOP MAGNITUDE

```
5.43  13.04  16.79   4.74  16.22  24.13  17.73   5.09   3.82  13.04   8.02   8.86   8.40   2.55   8.00
1.27   4.00   2.55  17.27  16.22   8.40   2.55   5.09  17.22  20.64  14.22  24.30   2.55  16.20   9.46
```

ENVELOP MAGNITUDE

```
4.77  11.22  16.45   3.24   9.43  16.18  16.45   7.87   3.82   7.67  12.58   8.40   3.24   1.27   2.00
1.27   2.00   2.55   6.00   2.55   2.00   2.55  10.00   6.36  10.00   2.00   2.55   6.00   2.55   2.00
```

RECEIVED CODE 16 SEQUENCE IS 1 1 0 1 FOLLOWED BY   CODBAR OR CODE FOR 1ST AND 2ND OUTPUTS RESPECTIVELY

ENVELOP MAGNITUDE

Table 3-6. Length 32 Code (5, 3) into Length 128 Code (6, 8, 6, 11) Crosscorrelation (Cont).

.32	2.00	1.27	2.00	6.00	3.82	6.00	6.00	6.36
.00	2.00	5.09	10.18	10.32	.00	11.22	11.22	.00

ENVELOP MAGNITUDE

.95	.00	.00	.00	.00	.00	.00	.00	.00
.00	.00	.00	.00	.00	.00	.00	.00	.00

RECEIVED CODE 16 SEQUENCE IS 1 1 1 0 FOLLOWED BY CODRAP OR CODE FOR 1ST AND 2ND OUTPUTS RESPECTIVELY

ENVELOP MAGNITUDE

1.32	4.00	1.27	4.00	6.00	5.09	1.27	4.00	7.64
6.36	12.00	16.05	13.04	9.48	5.09	16.05	13.04	5.09

ENVELOP MAGNITUDE

6.95	16.00	5.27	2.52	12.18	5.82	2.00	2.00	5.82
6.36	16.00	5.09	11.82	18.18	18.18	2.00	2.00	18.18

RECEIVED CODE 16 SEQUENCE 13 1 1 1 1 FOLLOWED BY CODDAP OR CODE FOR 1ST AND 2ND OUTPUTS RESPECTIVELY

ENVELOP MAGNITUDE

4.14	7.47	16.05	8.86	10.32	16.05	14.90	5.47	10.31
5.09	10.00	2.55	18.71	7.67	7.64	18.71	5.47	7.64

ENVELOP MAGNITUDE

4.77	9.48	16.20	9.43	16.20	16.20	9.48	5.00	16.20
5.09	6.00	2.55	9.43	16.20	7.64	8.00	5.00	7.64

MEAN   VAR   PEAK   PEAKS GT 18
                          OUT OF 1024

V.507   56.562   32.899   110

The MSKCOR program is set up to correlate a 2-bit length signal with a 1-bit length correlator (matched SAWD) with both the signal and the correlator bits having identical number of chips. Therefore, the first 64 chips of the incoming signal are correlated. As the first two chips exit the correlator, another two chips are added from the remaining longer string of the long signal and again subjected to the MSKCOR program. Note that whenever 64 chips of the input signal (equivalent to twice the length of the correlator) are correlated with a 32-chip coded SAWD, the program would normally print out 97 chip correlation points of the envelope magnitude of the baseband correlation curve. Note that one extra correlation point occurs because one chip delay on one of the correlator quadrature channels takes care of one chip staggering between the two quadrature channels of the MSK signal. The 32 end points out of a total of 97 correlation points are ignored as they correspond to the condition of the 64-chip signal followed by no signal.

Therefore, only the first 65 (97 minus 32) correlation points are printed out. As the two extra chips are added to compensate for the two exiting chips (implying that a new pair from the 64-length code pair is added for one pair leaving), the two new correlation points are printed for each new arrival of two chips. There are 188 distinct correlation points in addition to the 65 already described which are pointed out. The mean, variance, and peak are compared for each set of codes being correlated.

Table 3-7 summarizes the crosscorrelation of the 3 long codes into the 13 short codes under investigation. Table 3-7 provides a typical computer listing of the crosscorrelation side lobes because of a preferred set. The mean. variance, and the peak of the set correlated are printed out at the bottom line of table 3-8.

3.6   CODE SELECTION

Referencing tables 3-5 and 3-7, it is apparent that the short code (5, 3) and the long code (6, 8, 6, 11) result in low crosscorrelation side lobes. Although there are other codes under each crosscorrelation category that give slightly lower peak values of side lobes, these codes are not suitable when both categories of crosscorrelation are combined; that is, when crosscorrelation of the low data rate into high data rate and the high data rate into the low data rate are considered simultaneously. Therefore, the best Golay code pairs for the MSK application in a dual data rate system are the following:

  High Data Rate Code; (5, 3)

  Low Data Rate Code: (6, 8, 6, 11)

Table 3-9 lists, for reference, the (5, 3) code along with its C C * C mode of autocorrelation, and table 3-10 lists the (5, 3) code with its C $\overline{C}$ * C mode of autocorrelation. A confirmatory plot of the (5, 3) code autocorrelation in the C C * C mode using FFT is provided in figure 3-4 to validate the baseband results using the model baseband approach of Packet Radio Temporary Note No. 93. Notice that the envelope of this plot matches with the peak-to-peak envelope at every chip as predicted by the referenced model.

Tables 3-11 and 3-12 list the C C * C and the C $\overline{C}$ * C mode of autocorrelation for the long (6, 8, 6, 11) code selected.

Table 3-7. Low Data Rate Code (Length 128) into High Data Rate Code (Length 32) Crosscorrelation.

16 CODE	64 CODE 5, 3, 8, 3			64 CODE 5, 7, 6, 11			64 CODE 6, 8, 6, 11		
	PEAK	MEAN	PEAKS > 8	PEAK	MEAN	PEAKS > 8	PEAK	MEAN	PEAKS > 8
1, 1	16.0	5.3	47	16.2	5.27	43	16.15	5.1	55
1, 2	14.0	5.4	56	.1	5.0	38	16.1	5.4	45
1, 6	18.0	5.2	52	2	5.3	46	14.2	5.273	54
2, 8	14.3	5.3	63	16.2	5.3	59	16.37	5.0	55
3, 5	18.5	5.28	44	17.2	5.29	42	17.2	5.5	49
3, 7	20.1	5.48	60	12.59	5.2	42	14.2	5.6	56
5, 2	18.0	5.3	52	16.2	4.7	51	16.2	4.7	55
5, 3	16.2	5.3	50	12.2	5.48	74	12.59	5.1	65
5, 4	20.16	4.98	49	16.45	4.88	57	16.45	5.44	68
5, 7	16.0	4.7	40	16.0	5.5	60	12.69	4.9	50
5, 8	14.29	5.3	51	16.15	5.17	48	16.15	5.34	51
6, 2	16.00	5.56	54	16.08	4.53	40	18.0	5.32	60
6, 7	18.2	5.08	63	14.23	5.25	49	16.154	5.44	52

Table 3-8. Crosscorrelation, Length 128 Code (6, 8, 6, 11) into Length 32 Code (5, 3).

CODE 64(6, 8, 6,11)-CODE 16(5, 3)

ENVELOP MAGNITUDE

Table 3-8. Crosscorrelation, Length 128 Code (6, 8, 6, 11) into Length 32 Code (5, 3) (Cont).

Table 3-8. Crosscorrelation, Length 128 Code (6, 8, 6, 11) into Length 32 Code (5, 3) (Cont).

	MEAN	AVAR
80	4.7	8.7
81	6.1	4.0
82	6.1	3.5
83	4.0	2.2
84	6.0	4.1
85	6.1	4.6
86	3.0	1.9
87	4.0	2.9
88	6.1	3.5
89	5.9	2.2
90	4.7	2.7
91	4.7	2.5
92	6.1	6.1
93	1.3	4.6
94		6.2

MEAN	AVAR	PEAK	PEAKS GT 6
5.136	6.020	12.593	65

Table 3-9.   High Data Rate (Length 32) C C * C Correlation.

	M1	M2	M3	M4	MEAN	VARIANCE	PEAK
	5	3	0	0	7.63	5.10	8.00

CODE X

CODE Y

RXX*RYY

ENVELOP MAGNITUDE PEAK TO PEAK

Table 3-10.   High Data Rate (Length 32) C C̄ * C Correlation.

M1	M2	M3	M4	MEAN	VARIANCE	PEAK
5	3	0	0	2.44	4.35	6.00

CODE X

1   0   1   1   0   1   1   0   1

CODE Y

1   0   1   1   1   0   1   0

RXX*RYY

ENVELOP MAGNITUDE PEAK TO PEAK

Figure 3-4.   Autocorrelation (C C * C) of High Data Rate (5. 3)
Code Using Fast Fourier Transform (FFT).

Table 3-11.   Low Data Rate (Length 128) C C * C Correlation.

	MEAN	VARIANCE	PEAK
	6.24	24.69	16.00

M4 11
M3 6
M2 8
M1 6

CODE X

CODE Y

RXX*RYY

Table 3-11.   Low Data Rate (Length 128) C C * C Correlation (Cont).

ENVELOP MAGNITUDE PEAK TO PEAK

Table 3-12.   Low Data Rate (Length 128) C C̄ * C Correlation.

Table 3-12. Low Data Rate (Length 128) C $\bar{C}$ * C Correlation (Cont).

ENVELOP MAGNITUDE PEAK TO PEAK

3.7 SUMMARY OF RESULTS

Based on the data derived in the preceding paragraphs, the following important results are summarized:

a. High Data Rate (32-Chip Length)

Peak Autocorrelation Side lobe (C C * C) = 8.00

Mean Autocorrelation Side lobe (C C * C) = 2.63

Variance of Autocorrelation Side lobe (C C * C) = 5.10

Peak Autocorrelation Side lobe (C $\overline{C}$ * C) = 6.00

Mean Autocorrelation Side lobe (C $\overline{C}$ * C) = 2.44

Variance of Autocorrelation Side lobe (C $\overline{C}$ * C) = 4.35

Peak Crosscorrelation Side lobe
(due to low data rate code) = 12.59

Mean Crosscorrelation Side lobe
(due to low data rate code) = 5.14

Variance of Crosscorrelation Side lobe
(due to low data rate code) = 8.82

Ratio of Autocorrelation Peak to the Peak Autocorrelation
Side lobe (C C * C) = 12.04 dB

Ratio of Autocorrelation Peak to the Peak Autocorrelation
Side lobe (C $\overline{C}$ * C) = 14.54 dB

Ratio of Autocorrelation Peak to the Mean Autocorrelation
(C C * C) Side lobes = 21.70 dB

Ratio of Autocorrelation Peak to the Mean Autocorrelation
(C $\overline{C}$ * C) Side lobe = 22.36 dB

Ratio of Autocorrelation Peak to the Peak Crosscorrelation
Side lobe = 8.1 dB

Ratio of Autocorrelation Peak to the Mean Crosscorrelation
Side lobe = 15.96 dB

b. Low Data Rate (128-Chip Length)

Peak Autocorrelation Side lobe (C C * C) = 16.0

Mean Autocorrelation Side lobe (C C * C) = 6.24

Variance of Autocorrelation Side lobe (C C * C) = 24.69

Peak Autocorrelation Side lobe (C $\overline{C}$ * C) = 18.0

Mean Autocorrelation Side lobe (C $\overline{C}$ * C) = 5.11

Variance of Autocorrelation Side lobe (C $\overline{C}$ * C) = 22.28

Peak Crosscorrelation Side lobe (due to high data rate code) = 32.9

Mean Crosscorrelation Side lobe (due to high data rate code) = 9.5

Variance of Crosscorrelation Side lobe (due to high data rate code) = 56 56

Ratio of Autocorrelation Peak to the Peak Autocorrelation Side lobe
(C C * C) = 18.06 dB

Ratio of Autocorrelation Peak to the Peak Autocorrelation Side lobe
(C $\overline{C}$ * C) = 17.04 dB

Ratio of Autocorrelation Peak to the Mean Autocorrelation Side lobe
(C C * C) = 26.24 dB

Ratio of Autocorrelation Peak to the Mean Autocorrelation Side lobe
(C $\overline{C}$ * C) = 28.0 dB

Ratio of Autocorrelation Peak to the Peak Crosscorrelation Side lobe
= 11.8 dB

Ratio of Autocorrelation Peak to the Mean Crosscorrelation Side
lobe = 22.6 dB

REFERENCE

1. Alsup, J.M. , "Acoustic Surface Wave Golay Coded Matched Filters,"
    Naval Undersea Center Report # NUC-TN-981, San Diego, California, March 1973.

4.1 INTRODUCTION

The term "capture" has been defined to be a property of a receiver which measures its capability to distinguish one signal from an ensemble of several signals. The network simulation model developed by Network Analysis Corporation(N.A.C.) assumes zero capture; ie, if two or more packets impinge on a receiver, none are recovered. The receiver being developed by Collins for the experimental system does have a measure of capture capability and the purpose of this note is to describe this property. The intent is for the capture phenomenon to be added to the N.A.C. model with the objective of providing additional reality to their simulations.

To begin a description of the capture model, it is necessary to first characterize the receiver. Insofar as capture is concerned, there are four basic characteristics that describe the state of a receiver. These are:

a. Whether the receiver is in the receive enable mode

b. If in the receive enable mode, whether the receiver is in a synchronization period or a packet reception period

c. The number of packets available to be captured at the receiver

d. The specific characteristics of these packets.

The first characteristic only indicates whether the radio is in receive mode. Since it is a half-duplex operation, the radio can be in either of two states: transmit or receive. The second characteristic determines whether a receiver is receiving a packet or looking for a packet preamble for synchronization. Once a packet has been synchronized to, then the process of synchronization will not occur again until this packet has been completely received. The third and fourth characteristics define how many packets are available for reception and their specific nature. The parameters that completely describe a packet for the capture model are the following:

a. Time of arrival of the packet at the receiver

b. Power level of the packet

c. The packet length

d. The data rate of the packet.

These four parameters are the only packet related parameters required to determine the successful capture of a packet.

Capture Model Description

4.1 INTRODUCTION

The term "capture" has been defined to be a property of a receiver which measures its capability to distinguish one signal from an ensemble of several signals. The network simulation model developed by Network Analysis Corporation(N.A.C.) assumes zero capture; ie, if two or more packets impinge on a receiver, none are recovered. The receiver being developed by Collins for the experimental system does have a measure of capture capability and the purpose of this note is to describe this property. The intent is for the capture phenomenon to be added to the N.A.C. model with the objective of providing additional reality to their simulations.

To begin a description of the capture model, it is necessary to first characterize the receiver. Insofar as capture is concerned, there are four basic characteristics that describe the state of a receiver. These are:

a. Whether the receiver is in the receive enable mode

b. If in the receive enable mode, whether the receiver is in a synchronization period or a packet reception period

c. The number of packets available to be captured at the receiver

d. The specific characteristics of these packets.

The first characteristic only indicates whether the radio is in receive mode. Since it is a half-duplex operation, the radio can be in either of two states: transmit or receive. The second characteristic determines whether a receiver is receiving a packet or looking for a packet preamble for synchronization. Once a packet has been synchronized to, then the process of synchronization will not occur again until this packet has been completely received. The third and fourth characteristics define how many packets are available for reception and their specific nature. The parameters that completely describe a packet for the capture model are the following:

a. Time of arrival of the packet at the receiver

b. Power level of the packet

c. The packet length

d. The data rate of the packet.

These four parameters are the only packet related parameters required to determine the successful capture of a packet.

4.2 ASSUMPTIONS

Before continuing the description, it seems appropriate to list the assumptions that simplify the model and, more importantly, focus the attention on the objective of modeling capture. The assumptions are:

a. The distances between all network elements are known.

b. The receiver has two detectors: one with data rate 100 kb/s and another at 400 kb/s with processing gains of 128 and 32, respectively, that operate simultaneously.

c. No multipath phenomenon is considered.

d. No other sources of interference other than Gaussian noise and packets are considered.

e. The time that the receiver is transferred to receive enable is known.

The description of the capture model is divided into three parts. The first describes the calculations of packet parameters. The second presents the operation of the synchronization mode, and the third gives the operation of the reception mode. Some suggestions for implementation of the model into the N.A.C. simulation program are given; however, the total implementation is not included.

4.3 PACKET CHARACTERISTICS

It has been assumed that the packet originations and their time of origination are known. In the N.A.C. model, this is obtained from an event generator. The two significant independent variables are thus the coordinates of the transmitter of a packet and the time of transmission. From these two variables, one can then determine the time of arrival of this packet to any element of the network and the signal level of the packet at all the elements in the network. The derived signal level at each element's receiver is determined from a propagation attenuation calculation. This calculation is made assuming line of sight for repeater-repeater links. For repeater-terminal links, the propagation attenuation is based on Okumura, et al[1], propagation data which is described in detail in the appendix.

The time of arrival is based simply on free space delay of propagation. The data rate is implied in the fact that it is known which element transmitted and the intended receiver. That is, terminal-repeater and repeater-terminal transfers are 100 Kb/s, while repeater-repeater transfers are 400 Kb/s. The packet length is another known parameter obtained from the event generator; and for simplicity, it might be assumed that all packets are of fixed length.

4.4 SYNCHRONIZATION MODE

With the description of the derived packet characteristics complete, the question "How does the receiver sift through these available packets with varying characteristics and identify a specific packet?" can be addressed. The answer to this question begins with the synchronization process.

It has been pointed out that packets have a minimum amount of information associated with them that uniquely describes their state. This can be viewed as a multiple dimensioned vector defining a packet with the following components: To, From, Arrival time, Power level,

---

[1]The reference is given at the end of the appendix.

Length. The synchronization process is the alignment of the timing of the receiver and a particular packet and the subsequent discrimination by the receiver against all other packets. It is based on the operation of the bit synchronization circuitry, which works in the following way.

The bit synchronization circuit consists of a phase-lock loop with a coarse and a fine tracking ability. When a detector in the receiver is enabled, its bit synchronization circuit is free-running and generating three windows defined as Advance, Retard, and Sync. The envelope-detected correlation peaks coming out of the matched filters are summed together and a determination is made as to which window has the largest signal residing in its interval. If a signal is stronger by a factor of 3 dB than any other packet, the loop will slew in the advance or retard direction to center the synchronization window over this larger signal. If this signal continues to be larger than any other combination of signals found in the Advance or Retard window for a period of 10 bit intervals, then the in-lock condition is invoked. This condition narrows the Sync window down from $6T_c$ to $2T_c$ (T_c is period of chip) and enables the preamble detector.

Also, the stronger signal must not coincide in its correlation peak with other packet correlations within $2T_c$. Therefore, the time of arrivals of this signal and all other packet arrivals must be divisible by the bit interval, and the remainder of this division must be greater than $2T_c$ to ensure proper discrimination of the packets. Physically, this means that the time of arrival of the correlation peaks from the desired packet must be separated by at least $2T_c$ from the arrival times of any correlation peaks from other packets. If this is not the case, then the end of preamble will be assumed to go undetected. The bit synchronization circuit will continue to lock up to this signal as long as it is the larger signal.

It must be remembered that the receive enable condition could have been obtained at a point in the middle of the strongest signal packet in which its preamble has already been transmitted. Therefore, the end of preamble will not be detected. After a time-out period of 38 bit intervals, the synchronization circuit will unlock and will return to the hunting mode. This means that the successful detection of end of preamble (EOP) requires that the strongest signal must reach the lock condition of being greater than any other packet within $35T_b$ or less of its initial arrival time to ensure that the preamble is detected. Another simplifying assumption can be made that only packets at one data rate compete for synchronization. This means that 100-kb/s packets are compared for synchronization into 100-kb/s data detector but not 400-kb/s packets and vice versa. Figure 4-1 shows a flow chart of synchronization.

4.5 PACKET RECEPTION

If it is assumed that the receiver has synchronized to one packet and the detection decision is made within a $2T_c$ window, then an expression of the signal-to-noise ratio out of the matched filter can be obtained. This relation reflects the time discrimination. The general equation is:

$$SNR = \frac{2KS_1}{N_oR_c + \sum_{m=2}^{M} KS_m \, p_{1,m}^2}$$
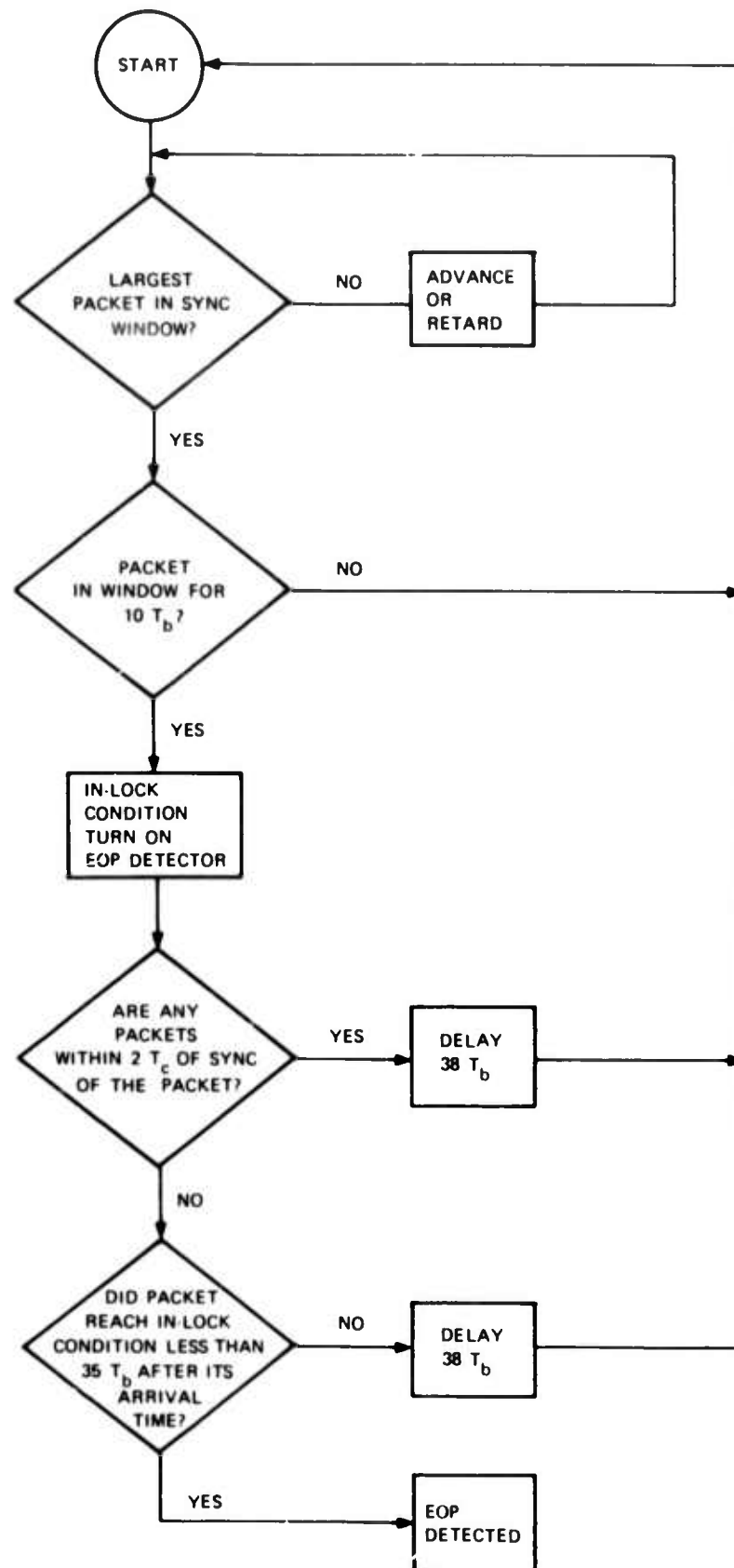
Figure 4-1.   Synchronization Process Flow Diagram.

where

S_1 =   Power level of synchronized packet signal

K =   Spread factor (number of chips per bit) for this given detector

$N_o R_c$ =   Thermal noise power (constant)

S_m =   Power level of mth packet

$\overline{P_{1,m}^2}$ =   Normalized crosscorrelation value in $2T_c$ window of S_1 PN sequence and and S_m PN sequence

M =   Number of available packets at the receiver

The power levels of the ensemble of packets impinging on the receiver are known, along with the value of K which is 128 for the 100-kb/s data rate and 32 for the 400-kb/s data rate, depending on the S_1 data rate. The noise power is constant and equal to $N_o R_c$ adjusted by the noise figure of the receiver (8 dB). The normalized crosscorrelation coefficient $\overline{P_{1,m}^2}$ is dependent on the codes and their time displacement. For example,

$$\overline{P_{LL}^2}(\tau) = \begin{cases} 1 & \text{if } |\tau| < 2T_c \\ \dfrac{63}{(128)^2} & \text{if } |\tau| \geq 2T_c \end{cases}$$

where

$\overline{P_{LL}^2}$ = Normalized crosscorrelation of low data rate code with itself and represents the displacement of correlation peaks.

The value of $\overline{P_{LL}^2}$ out of synchronization was obtained through computer simulation of the selected codes. Other crosscorrelation combinations are:

$$\overline{P_{HH}^2}(\tau) = \begin{cases} 1 & \text{if } |\tau| < 2T_c \\ \dfrac{12}{(32)^2} & \text{if } |\tau| \geq 2T_c \end{cases}$$

$$\overline{P_{LH}^2}(\tau) = \frac{35}{(32)^2} \quad \text{for all } \tau$$

$$\overline{P_{HL}^2}(\tau) = \frac{146}{(128)^2} \quad \text{for all } \tau$$

where

$\overline{P_{HH}^2}$ is crosscorrelation of high data rate code with itself

$\overline{P_{LH}^{2}}$ is crosscorrelation of low data rate code into high data rate matched filter

$\overline{P_{HL}^{2}}$ is crosscorrelation of high data rate code into low data rate matched filter

The determination of τ, which is only important in $\overline{P_{LL}^{2}}$ and $\overline{P_{HH}^{2}}$, is obtained from the arrival times of packet m and the synchronized packet. The relation is:

$$\tau = \text{fractional part } \frac{|T_{m} - T_{1}|}{T_{b}}$$

where

T_{b} = 10 microseconds for low data rate
2.5 microseconds for high data rate

T_{m} = Arrival time of packet m

T_{1} = Arrival time of packet 1 (synchronized)

It should be remembered that $2T_{c} = 156 \times 10^{-9}$ seconds.

This SNR will vary as events take place that impact the receiver and as packets terminate; therefore, the signal-to-noise ratio should be recalculated each time this happens and a weighted average obtained based on the time between events.

The average signal-to-noise ratio is then used to obtain the probability of a bit error (P_{e}).

The probability of bit error as a function of signal-to-noise ratio for differentially coherent MSK is:

$$P_{e} = (1/2)e^{-SNR/2}$$

and is shown graphically in figure 4-2.

With a value of P_{e}, one can then determine the probability of success of a packet of length n bits from the equation:

$$P_{n} = (1 - P_{e})^{n}$$

The P_{n} provides the measure needed to determine if a packet is successfully received error free. A Monte Carlo method can be used to determine the success or failure of a packet reception. This could be the selecting of a random number between 0 and 1 from a uniform distribution with the test being that if this number, X, is greater than P_{n}, then the packet has one or more errors and is not successfully received. If X is less than P_{n}, then the packet has no errors and is successful.
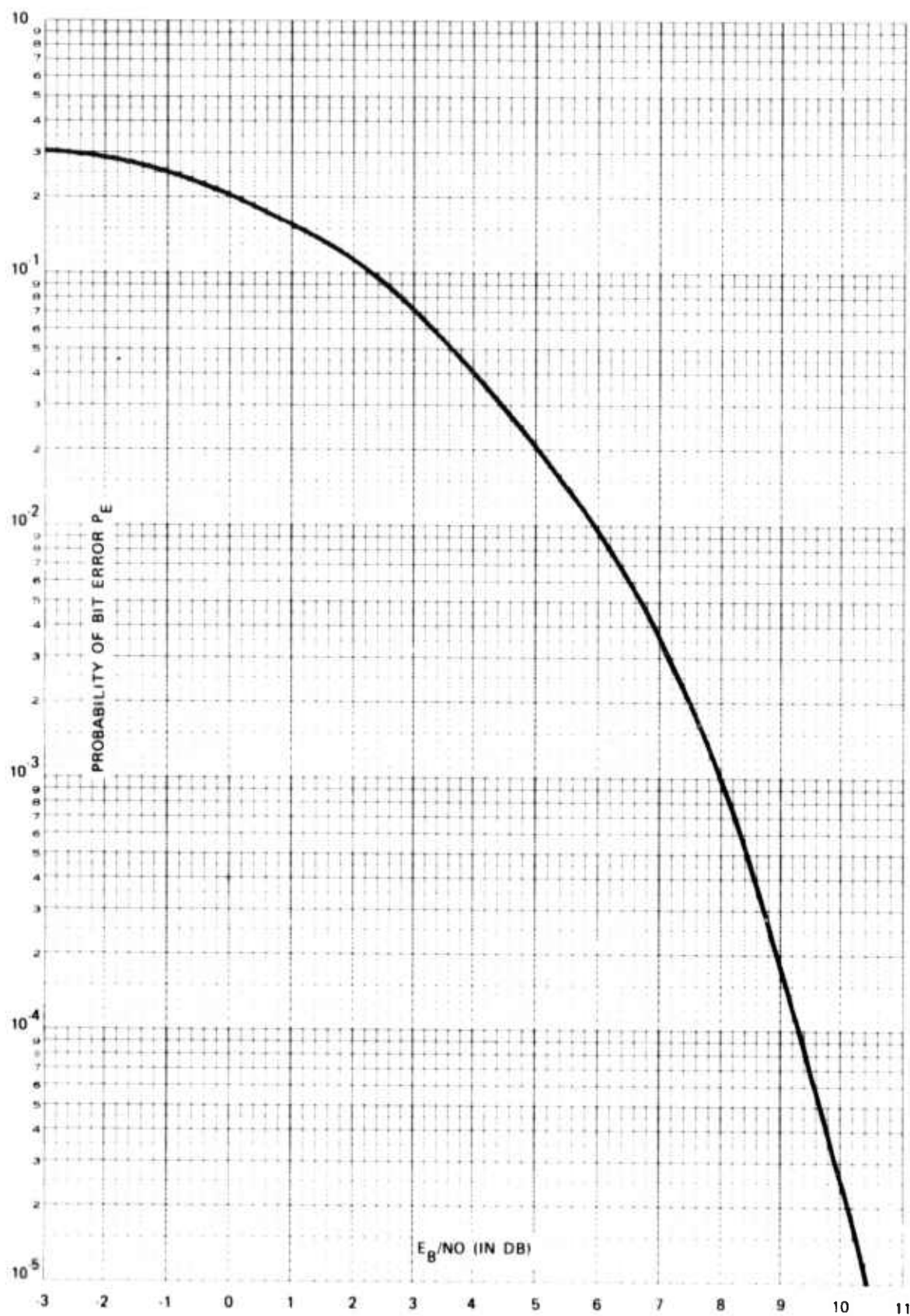
Figure 4-2. P_e Versus SNR Differentially Coherent MSK.

4.6   IMPLEMENTATION SUGGESTIONS

The capture phenomenon has been described as it takes place in the Collins design. This, however, very likely will not be an acceptable algorithm for the computer simulation network model due to its complexity. Therefore, reality will probably need to be tempered with practicality of implementation.

One suggestion is to partition the network such that not all element transmissions impact on all other network elements. The criteria of selection might be the elimination of packets from elements whose mean signal level approaches the thermal noise level. The signal level calculation through the propagation model and the synchronization model are basic to the capture ability; however, the packet reception model might be simplified by assuming no packets are synchronous with the synchronization packet and the $\overline{P_{1,m}^{2}}(\tau)$ terms are relatively very small. This means that the terms in the denominator of the SNR equation associated with other packets might be neglected and only one signal-to-noise ratio calculated for the packet transmission.

Okumura Path Loss Approximation

The following describes a computer algorithm which has been generated to incorporate Okumura's path loss attenuation data into the capture model for the N. A. C. packet radio simulation program. For this program, the average effective transmission heights for a repeater and a terminal were assumed to be 45 meters (148 feet) and 3 meters (9. 8 feet), respectively.

Figures A-1 and A-2 have been included to illustrate the process. Figure A-1 gives the Okumura path loss attenuation relative to free space, interpolated from Figure 10, pages 836-840 of Okumura, et al, for 1775 MHz with H_{te} = 45m and H_{re} = 3m. Figure A-2 gives an approximation of figure A-1, where Okumura's median attenuation (in dB) relative to free-space loss as a function of distance is given by:

$$A_{FS} = [(\log_{10}d)\ (4)/(\log_{10}2)] + 33, \text{ for d} \leq 22.6 \text{ km},$$

or

$$A_{FS} = [(\log_{10}d)\ (12)/(\log_{10}2)] - 3, \text{ for d} > 22.6 \text{ km},$$

where

A_{FS} = Attenuation relative to free space

4 and 12 (in dB/octave) represent the slope of lines with zero points (log d = 0; ie, d = 1) at 33 and -3 dB, respectively.

The pivot point, or intersection of these two lines is 22. 6 km. This approximation is almost identical for d ≤ 15 km and d ≥ 30 km. For 15 < d < 30 km, the approximation is within 2 dB of Okumura's data.

However, the attenuation as given by Okumura is only a median value. Thus, per Figure 37 A, page 860 of Okumura, et al, a "correction" factor must be added to A_{FS}. This is accomplished by generating a random variate using a normal distribution with a mean of 0 and standard deviation of 5.

The total attenuation, as a function of distance and frequency is as follows:

Path loss attenuation (dB) = free space loss (dB) +
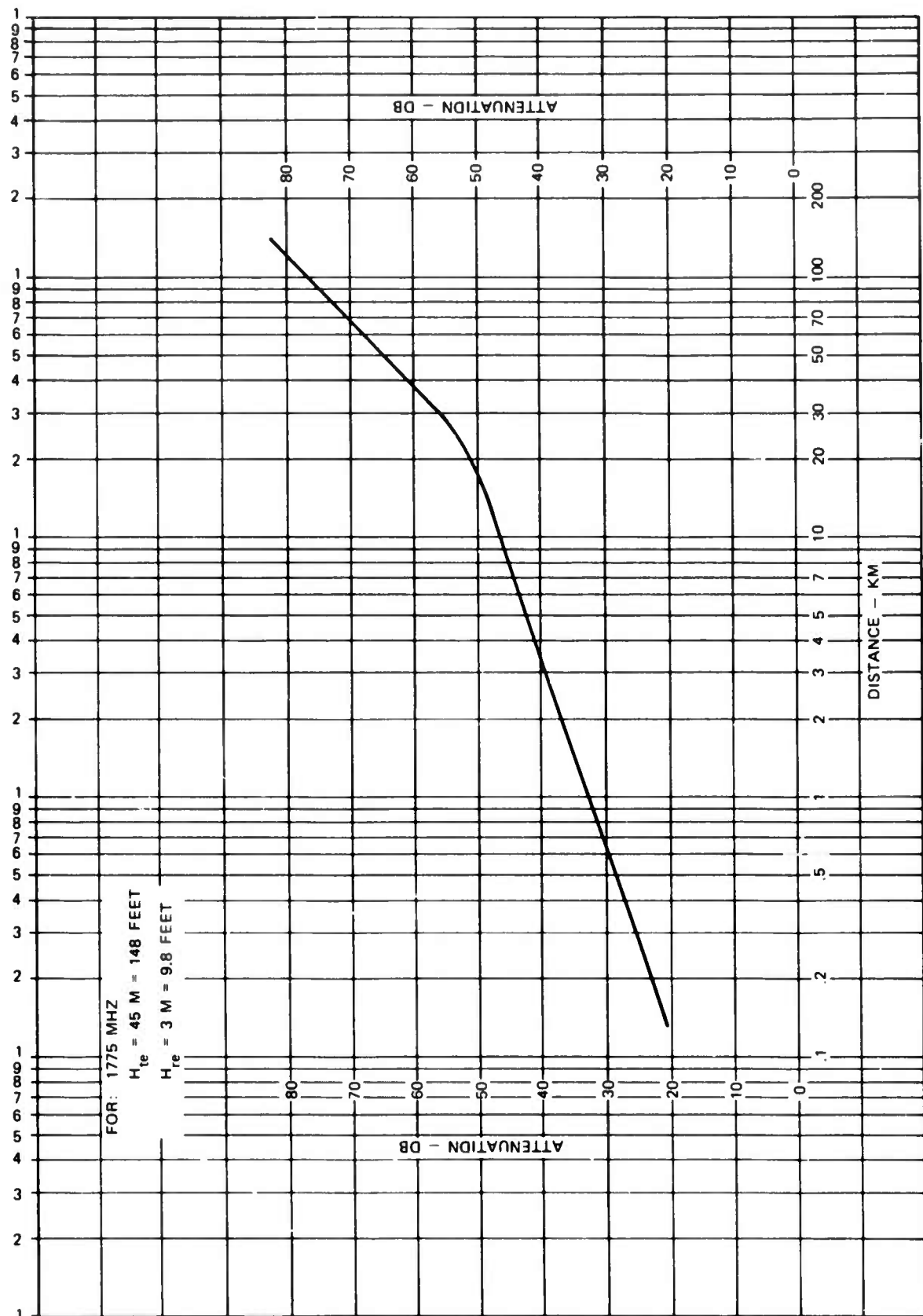
median Okumura (dB) +

correction (dB)

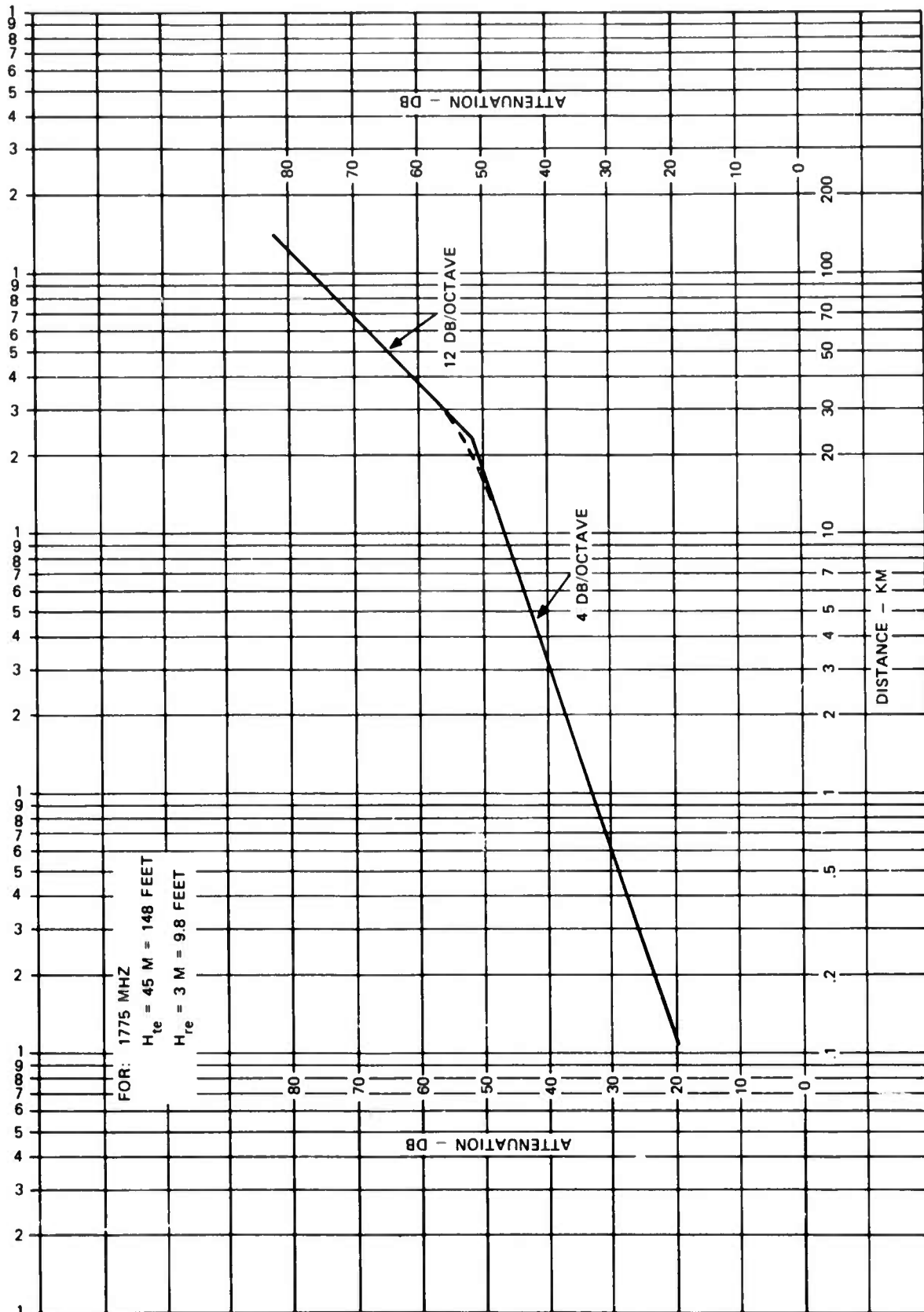Figure A-1.   Okumura Path Loss Attenuation (Relative to Free Space).

Figure A-2.   Approximate Okumura Path Loss Attenuation (Relative to Free Space).

Path loss attenuation $= 32.5 + 20 \log F + 20 \log D$

$$+ A_{FS} + X \sim n(x, \ 0, \ 5)$$

The slopes of the lines for figure A-2 are independent of changes in frequency. However, the slopes are dependent on the effective transmission height of the repeater. Even so, if an average effective transmission height can be assumed for the repeaters in the packet radio network, Okumura's data can be approximated for the N.A.C. simulation program.

A listing of the computer algorithm and sample input and output data follows. The program calculates the path loss attenuation for a given distance and frequency based on the above loss equation and provides a random component from a normal distributed random number generator. It is based on antenna heights of repeater and terminal of 45 meters and 3 meters, respectively. The only input data that the program requires is the frequency in megahertz and distance in miles.

THIS PROGRAM WILL CALCULATE THE PATH LOSS ATTENUATION (RELATIVE TO ISOTROPIC) FOR A
TRANSMITTED SIGNAL USING THE ATTENUATION DATA OF OKUMURA, ET. AL., ADJUSTED PER
OKUMURA BY A NORMALLY DISTRIBUTED RANDOM VARIABLE.

THE REPEATER EFFECTIVE TRANSMISSION HEIGHT IS ASSUMED TO BE 45 METERS = 148 FEET. THE
TERMINAL EFFECTIVE TRANSMISSION HEIGHT IS ASSUMED TO BE 3 METERS = 9.8 FEET.

```
REAL X(102) /102.0/
REAL DIST, DISTKM, FRESP, OKATEN, FREQ, XMEAN, STDEV, TOTATN
INTEGER NRAND, NUMB

      SET ALL USER SUPPLIED INPUTS—

                  DIST = REPEATER TO TERMINAL GROUND RANGE (MILES),
                  DISTKM = SAME AS DIST (KM), CALCULATED BY PROGRAM,
                  FREQ = TRANSMISSION FREQUENCY (MHZ),
                  XMEAN = MEAN OF RANDOM NUMBERS (DB),
                  STDEV = STANDARD DEVIATION OF RANDOM NUMBERS (DB),
                  NRAND = NUMBER OF RANDOM NUMBERS TO BE GENERATED,
                  X (1) = SEED NUMBER FOR THE RANDOM NUMBER GENERATOR.

DIST = 10.0
FREQ = 1775.0
XMEAN = 0.0
STDEV = 5.0
NRAND = 102
X (1) = (2.0835) − 1.0

      DO FOR DIST = 10 AND 40

DO 8 J = 1,2

                  CALCULATE THE FREE SPACE ATTENUATION (DB)

  FRESP = 36.6 + 20.0*ALOG10(FREQ) + 20.0*ALOG10(DIST)

                  CALCULATE THE OKUMURA ATTENUATION (DB) RELATIVE TO
                  FREE SPACE AS GIVEN BY FIGURE 10,  PAGES B36-40 OF
                  OKUMURA, ET. AL..

DISTKM = (DIST)*(1.609344)
IF (DISTKM .GT. 22.6) GO TO 1
OKATEN = ((ALOG10(DISTKM)*(4.0))/ALOG10(2.0)) + 33.0
GO TO 2
1  OKATEN = ((ALOG10(DISTKM)*(12.0))/ALOG10(2.0)) − 3.0
2  CONTINUE
IF (J .GT. 1) GO TO 3

                  GENERATE A NORMALLY DISTRIBUTED RANDOM VARIABLE TO
                  CORRECT THE OKUMURA ATTENUATION PER FIGURE 37 (A),
                  PAGE B60 OF OKUMURA, ET. AL..

                  THE FIRST 100 NUMBERS GENERATED WILL BE IGNORED.

  K = 100
```

CALCULATE THE TOTAL ATTENUATION (DB).

```
      K = K + 1
      TOTATN = FRESP + OKATEN + X (K)
```

WRITE THE TOTAL ATTENUATION.

```
      NUMB = K - 100
      IF (J .GT. 1) GO TO 6
      WRITE (7,4)
    4 FORMAT (1H1,//////)
      WRITE (7,5)
    5 FORMAT (10X,'NUMBER', 5X,'DISTANCE', 5X,'FREE SPACE', 5X,
     X        'OKUMURA', 5X,'RANDOM', 5X,'TOTAL ATTENUATION',//)
    6 WRITE (7,7) NUMB, DIST, FRESP, OKATEN, X(K), TOTATN
    7 FORMAT (12X, 1I1, 8X, 1F7.2, 7X, 1F7.2, 6X, 1F7.2, 5X, 1F7.2, 10X, 1F7.2,/)
```

RESET DIST.

```
      DIST = 40.0
    8 CONTINUE
      WRITE (7,4)
```

ALL DONE.

```
      STOP
      END
```

NUMBER	DISTANCE	FREE SPACE	OKUMURA	RANDOM	TOTAL ATTENUATION
1	10.00	121.58	49.03	-.20	170.42
2	40.00	133.63	69.10	-2.80	199.92

REFERENCE

1. Okumura, et al, "Field Strength And Its Variability In VHF and UHF Land-Mobile Radio Services," Review of the Electrical Communication Laboratory, Vol. 15, numbers 9-10, September-October 1968.